Supporting Information for the manuscript

Multielectron Redox Chemistry of Lanthanide Ions Supported by Tetradentate Schiff Bases.

Clément Camp, Valentin Guidal, Biplab Biswas, Jacques Pécaut, Lionel Dubois and Marinella Mazzanti*

Laboratoire de Reconnaissance Ionique et Chimie de Coordination, Service de Chimie Inorganique et Biologique (UMR-E 3 CEA-UJF, FRE 3200 CNRS), INAC,

CEA-Grenoble, 38054 GRENOBLE, Cedex 09, France.

Fax: (+)33(0)438785090 ; E-mail: marinella.mazzanti@cea.fr

*Correspondence to Dr. Marinella Mazzanti

Contents :

A) X-ray structural information for K_3[Tb(bis-salophen)]

B) ^{1}H NMR spectra

C) ES-MS spectra

D) UV-vis spectra

E) Electrochemistry data

A) Ortep of the solid state structure of K_3[Tb(bis-salophen)]

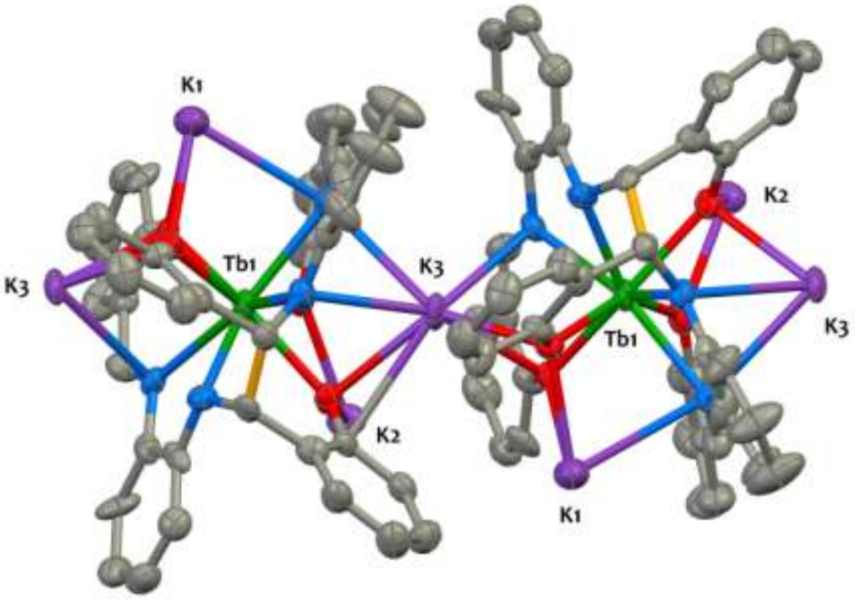

Figure S.A.1. Ortep view of the solid-state structure of $\{[K_3Tb(\text{bis-salophen})](py)_5\}_\infty$ **4**. Hydrogen atoms and solvent molecules are omitted for clarity. The C-C bonds formed by reduction of the imine moieties of the salophen ligands are represented in yellow. Color code: terbium (green), potassium (purple), nitrogen (blue), oxygen (red) and carbon (grey).

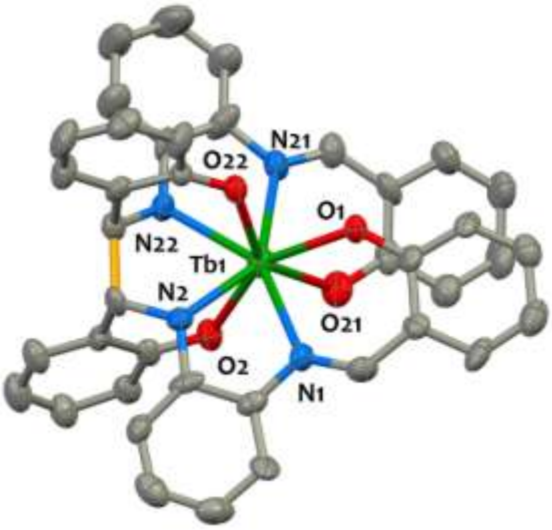

Figure S.A.2. Detail of the solid-state molecular structure **4** representing the $[Tb(\text{bis-salophen})]^{3-}$ anion. The C-C bond formed by reduction of the imine moieties of the salophen ligands is represented in yellow. Color code: terbium (green), nitrogen (blue), oxygen (red) and carbon (grey).

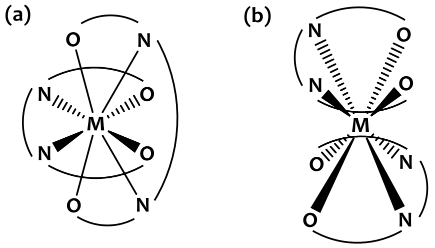

Figure S.A.3. Representation of the two isomeric forms of $[M(\text{salophen})_2]$ complexes. a) meridional isomer. b) sandwich isomer.

B) ^{1}H NMR spectra

Solution structure of K[Ln^R(salophen)$_2$]: The K[Ln^R(salophen)$_2$] complexes are stable and soluble in common organic solvants such as THF, pyridine, acetonitrile, and the recorded mass spectra are in agreement with this formulation in solution.

The ^{1}H NMR spectrum of the K[Nd(^{Me}salophen)$_2$] complex (Figure S.B.13) recorded in deuterated THF at room temperature shows two sets of seven signals in agreement with the presence in solution of the sandwich and meridional isomers in a ~ 1:2 ratio. The isomer ratio is solvent dependent (a ratio 1:1.4 is found in acetonitrile). The ^{1}H NMR spectrum of the K[Nd(salophen)$_2$] and K[Nd(^{tBu}salophen)$_2$] complexes (Figures S.B.1 and S.B.15) recorded in deuterated THF at room temperature displays a series of broad peaks suggesting the presence of exchanging solution species. The spectrum of K[Nd(^{tBu}salophen)$_2$] remains broad at low temperature (243 K), while the ^{1}H NMR spectrum of K[Nd(salophen)$_2$] recorded at 243 K in deuterated THF shows 14 resonances of equal intensity ranging from δ = 39.5 to δ -13.3 ppm (Figure S.B.2) in agreement with the presence of two isomers in a 1:1 ratio. The dynamic behaviour of the K[Ln(salophen)$_2$] complexes varies with the size of the Ln(III) ion with an increased rigidity observed for the smaller lanthanide ions (two sets of well resolved signals of equal intensity are observed for the Yb(III) complex at room temperature) (Figures S.B.8).

Figure S.B.1. ^{1}H NMR spectrum (298 K, 400 MHz) in THF-d_8 of a ~5 mM solution of K_2salophen and Nd(OTf)$_3$ in a 2:1 ratio affording K[Nd(salophen)$_2$].

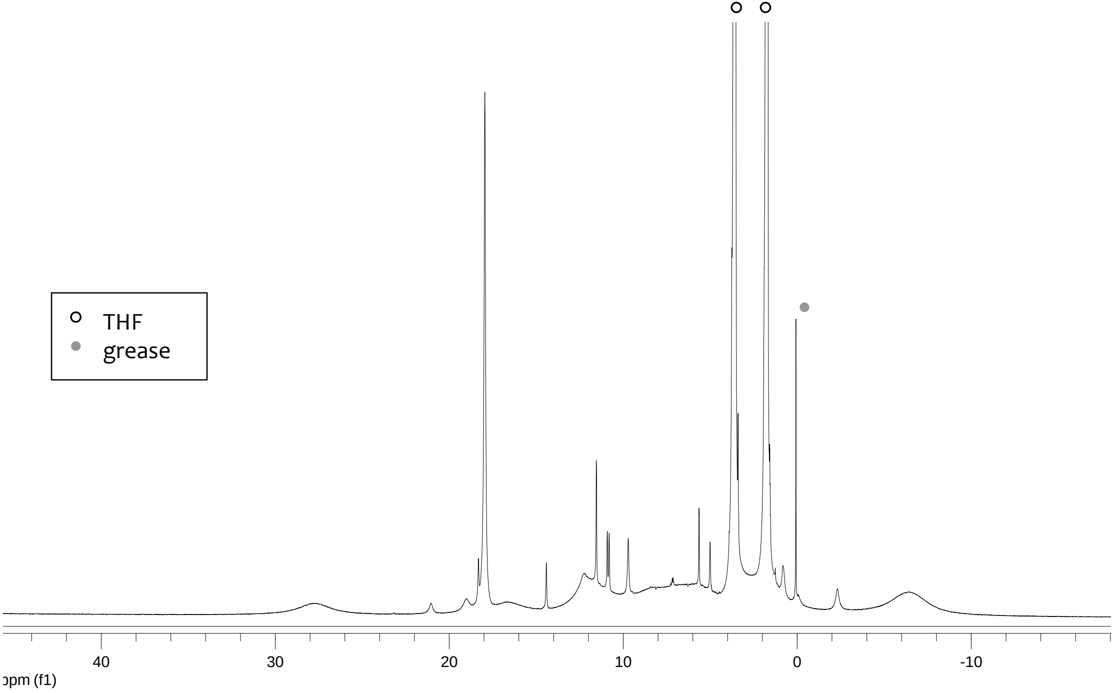

Figure S.B.2. ^{1}H NMR spectrum (243 K, 400 MHz) in THF-d_8 of a ~5 mM solution of K_2salophen and $Nd(OTf)_3$ in a 2:1 ratio affording $K[Nd(salophen)_2]$.

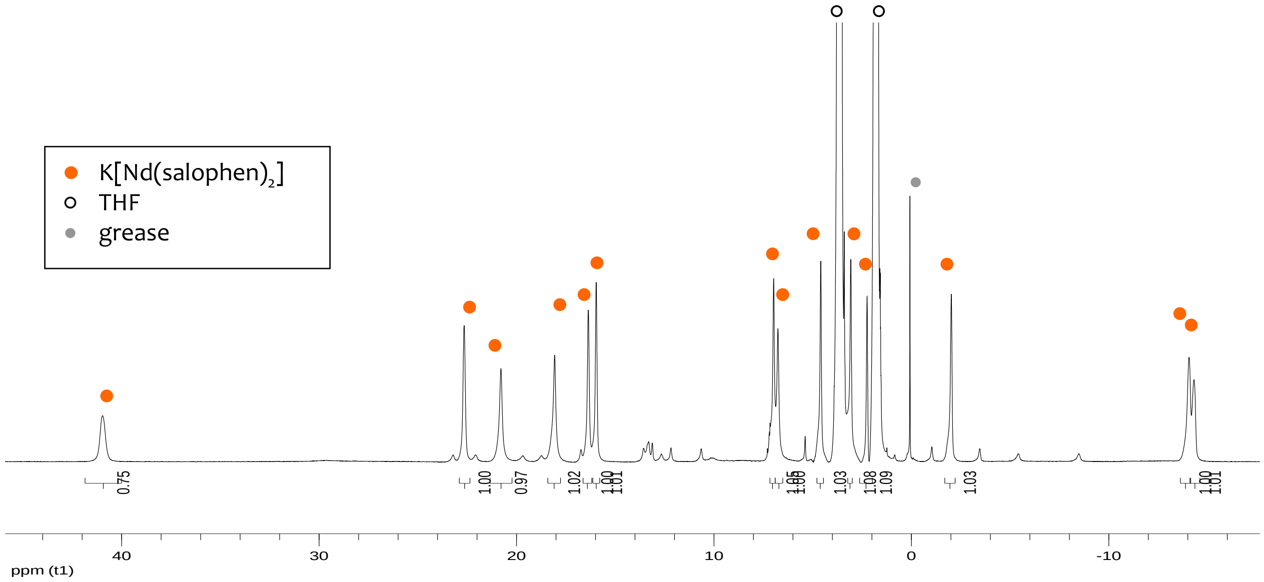

Figure S.B.3. ^{1}H NMR spectrum (298 K, 200 MHz) in THF-d_8 of the complex **$K_3[Nd(bis\text{-}salophen)]$**.

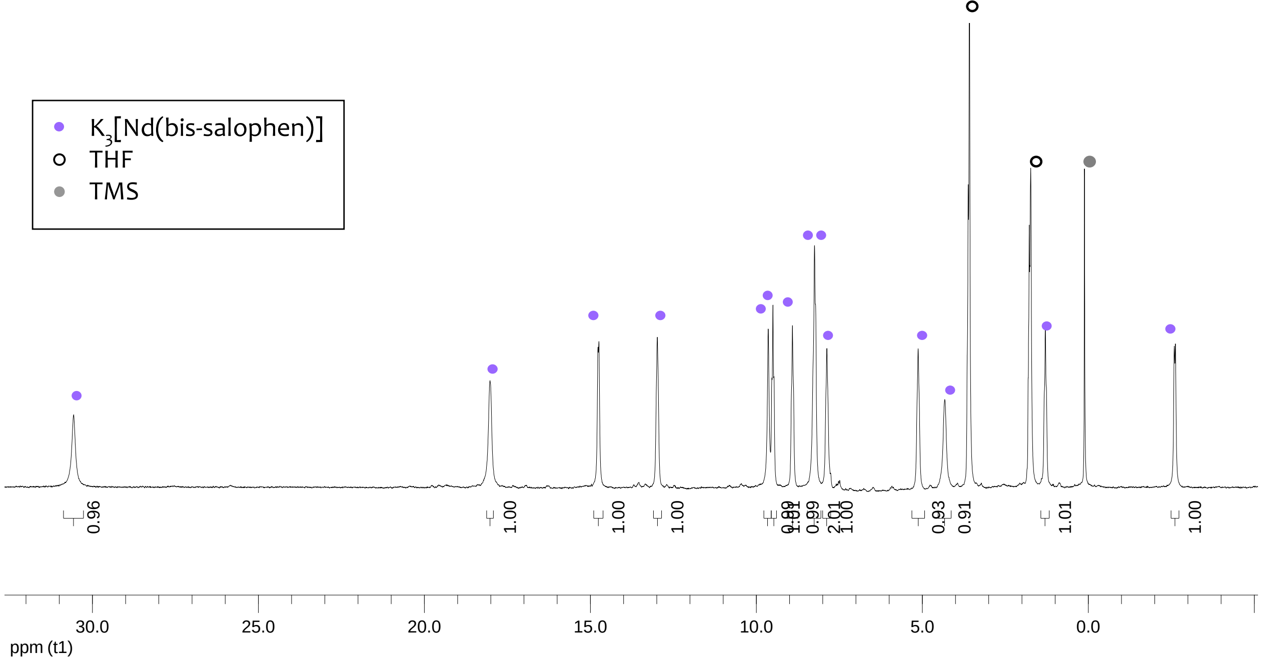

Figure S.B.4. ^{1}H NMR spectrum (293K, 200 MHz) in THF-d_8 of the complex **K[Eu(salophen)$_2$]**.

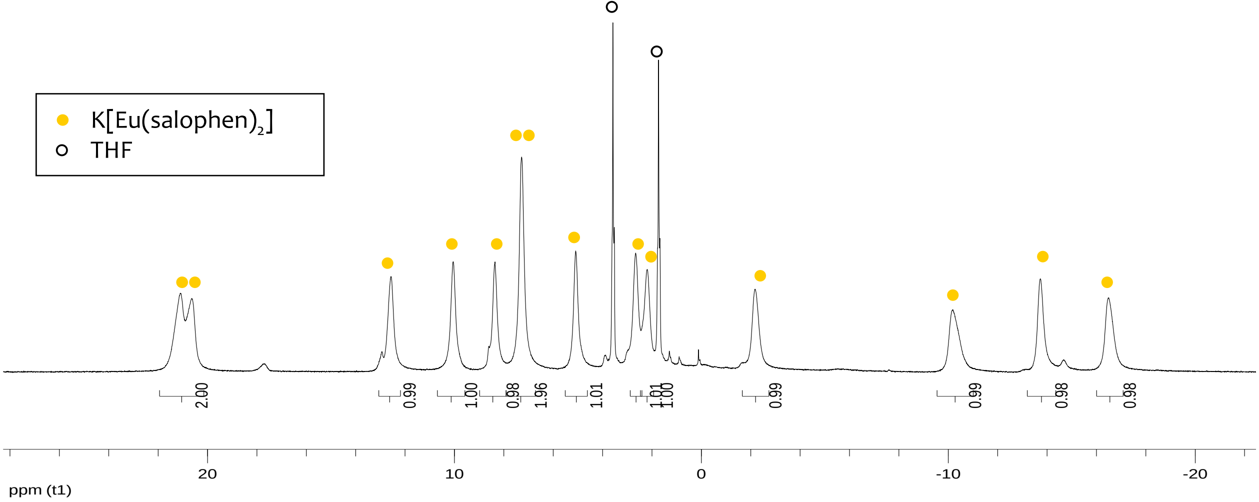

Figure S.B.5. ^{1}H NMR spectrum (293K, 200 MHz) in THF-d_8 of the complex **K$_3$[Eu(bis-salophen)]**.

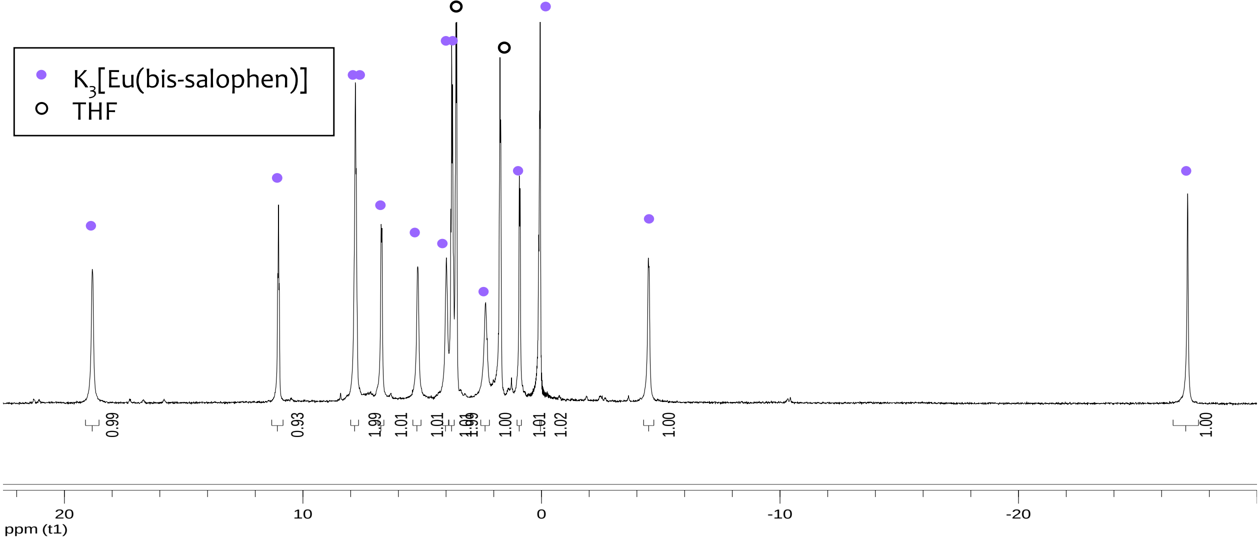

Figure S.B.6. ^{1}H NMR spectrum (273K, 400 MHz) in THF-d_8 of the complex **K[Tb(salophen)$_2$]**.

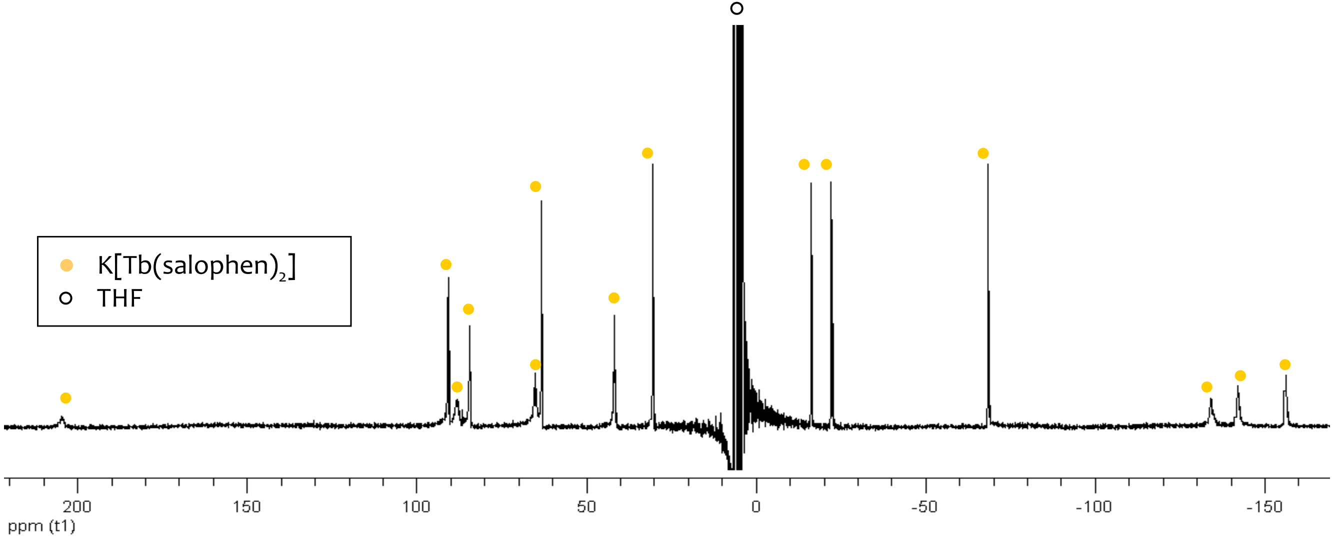

Figure S.B.7. ^{1}H NMR spectrum (298K, 400 MHz) in THF-d_8 of the complex **K$_3$[Tb(bis-salophen)].**

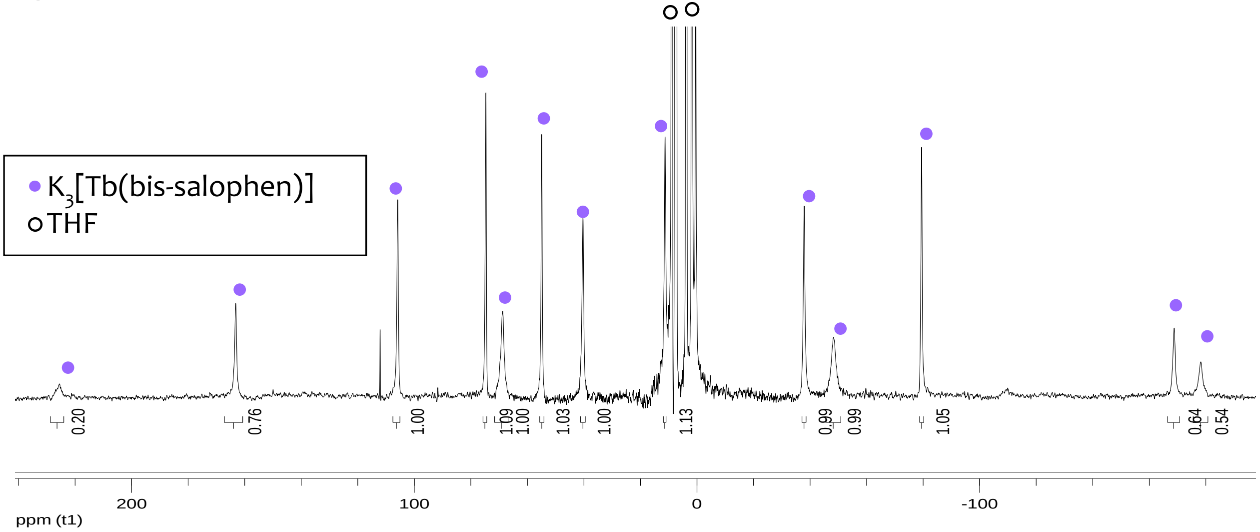

Figure S.B.8. ^{1}H NMR spectrum (298K, 400 MHz) in THF-d_8 of the complex **K[Yb(salophen)$_2$]**.

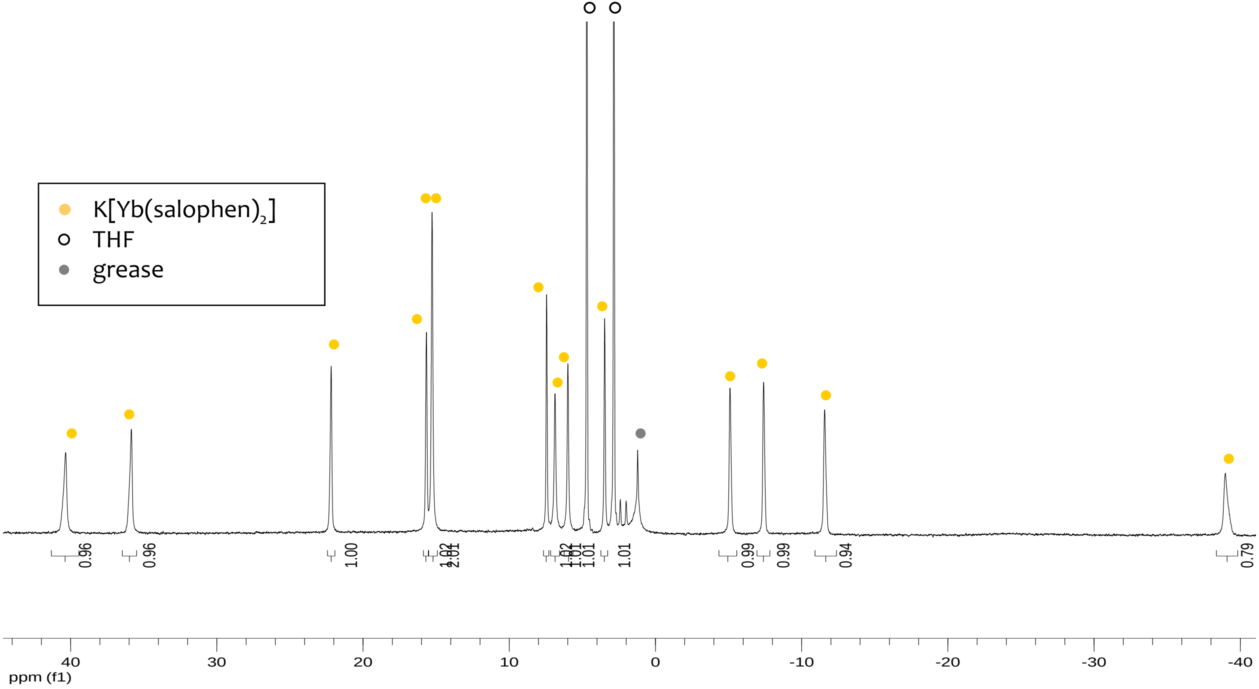

Figure S.B.9. ^{1}H NMR spectrum (243K, 400 MHz) in THF-d_8 of the complex **K$_3$[Yb(bis-salophen)]**.

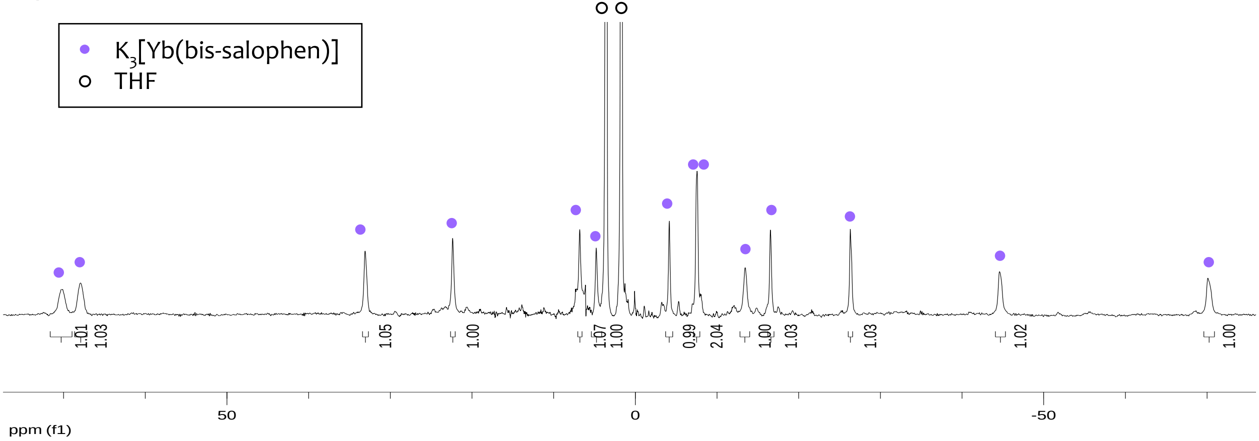

Figure S.B.10. ^{1}H NMR spectrum (298K, 400 MHz) in THF-d_8 of the reaction mixture of NdI_2 with 2 equivalents of K_2salophen a) before addition of K b) after addition of K. Yellow : K[Nd(salophen)$_2$] ; purple K_3[Nd(bis-salophen)].

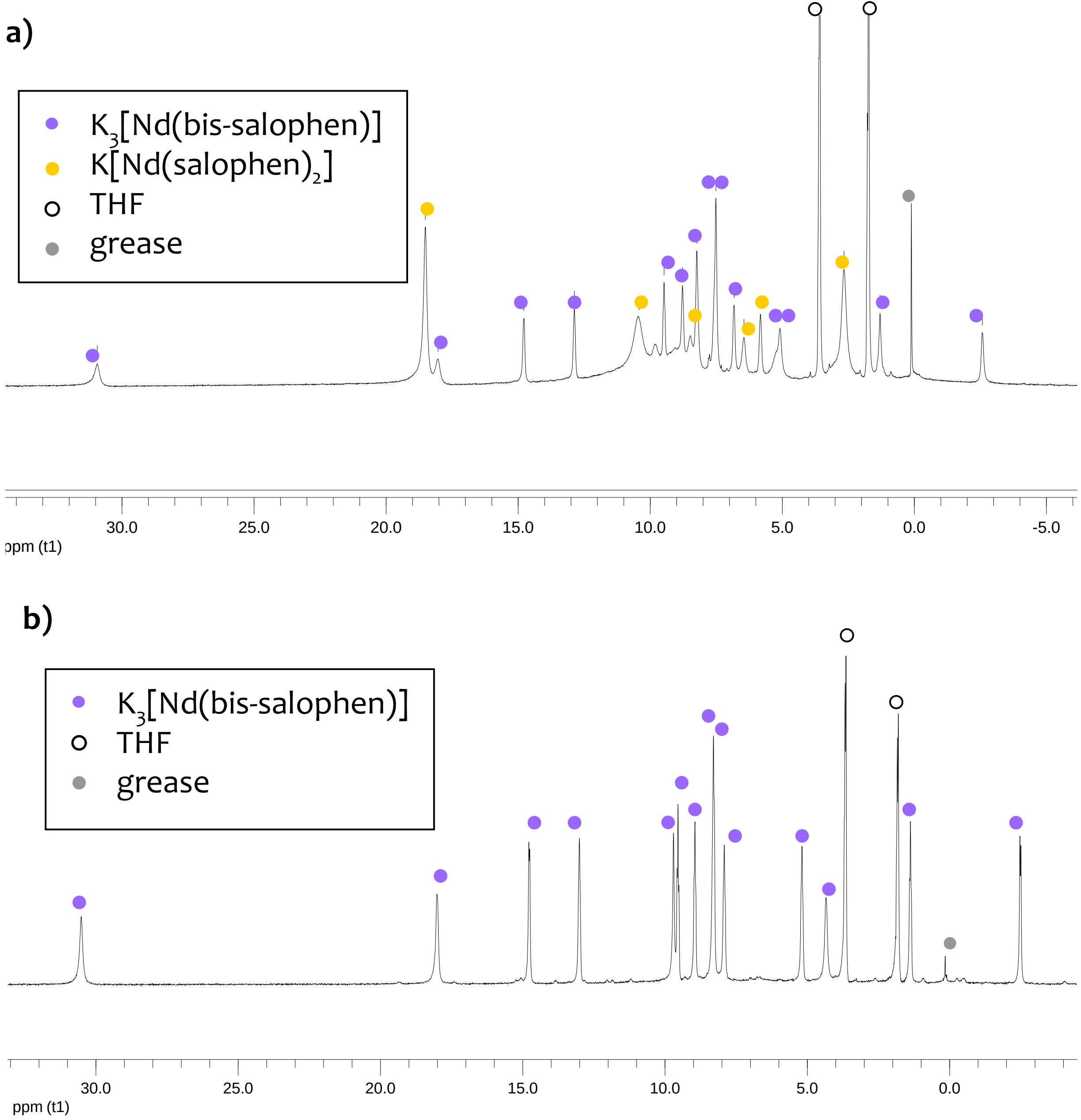

Figure S.B.11. ^{1}H NMR spectrum (298K, 400 MHz) in THF-d_8 of the reaction mixture of EuI_2 with 2 equivalents of K_2salophen : Yellow : **K[Eu(salophen)$_2$]** ; purple **K_3[Eu(bis-salophen)]**.

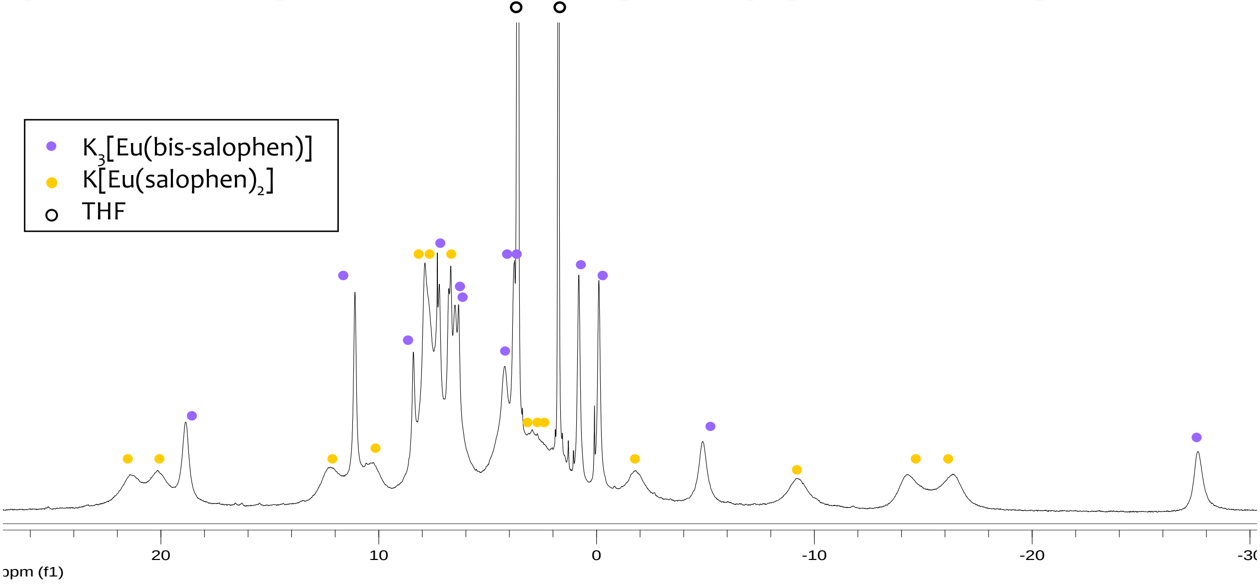

Figure S.B.12. ^{1}H NMR spectrum (243K, 400 MHz) in THF-d_8 of the reaction mixture of EuI2 with 2 equivalents of salophenK_2 : Yellow : **K[Eu(salophen)$_2$]** ; purple **K_3[Eu(bis-salophen)].**

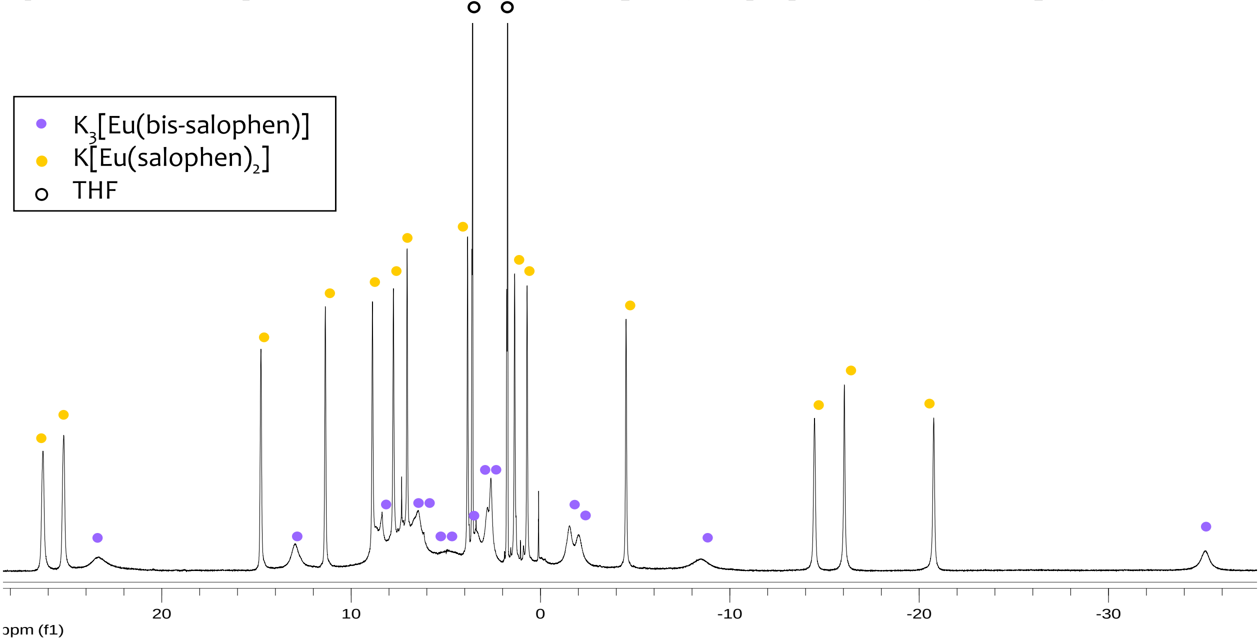

Figure S.B.13. ^{1}H NMR spectrum (298K, 200 MHz) in THF-d_8 of the complex **K[Nd(^{Me}salophen)$_2$]**.

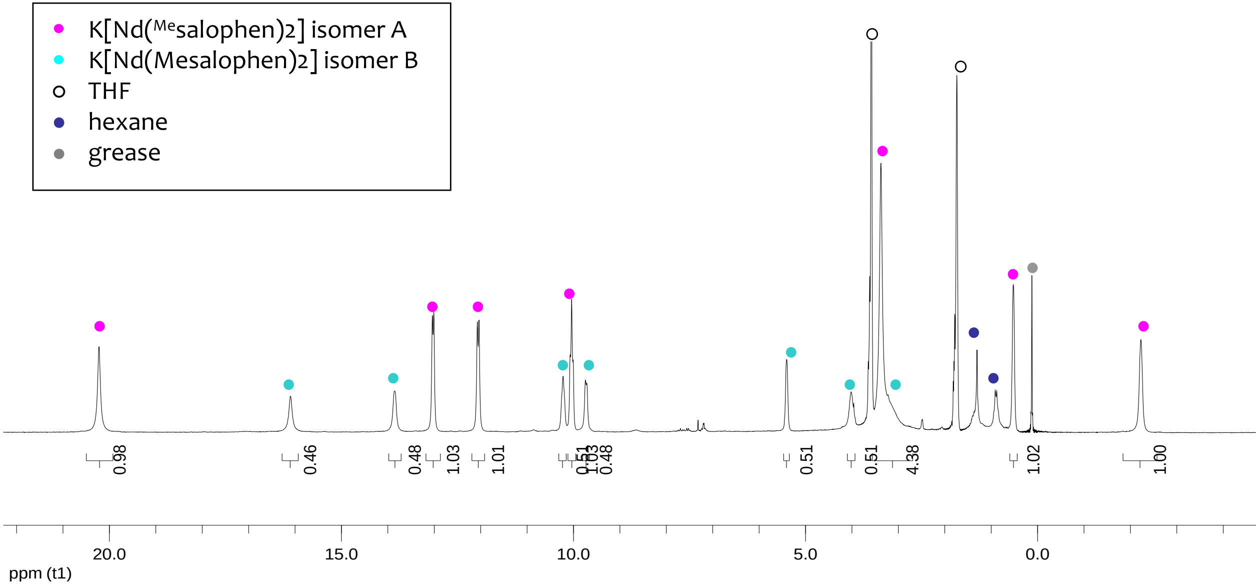

Figure S.B.14. ^{1}H NMR spectrum (298K, 200 MHz) in THF-d_8 of the complex **K_3[Nd(bis-^{Me}salophen)]**.

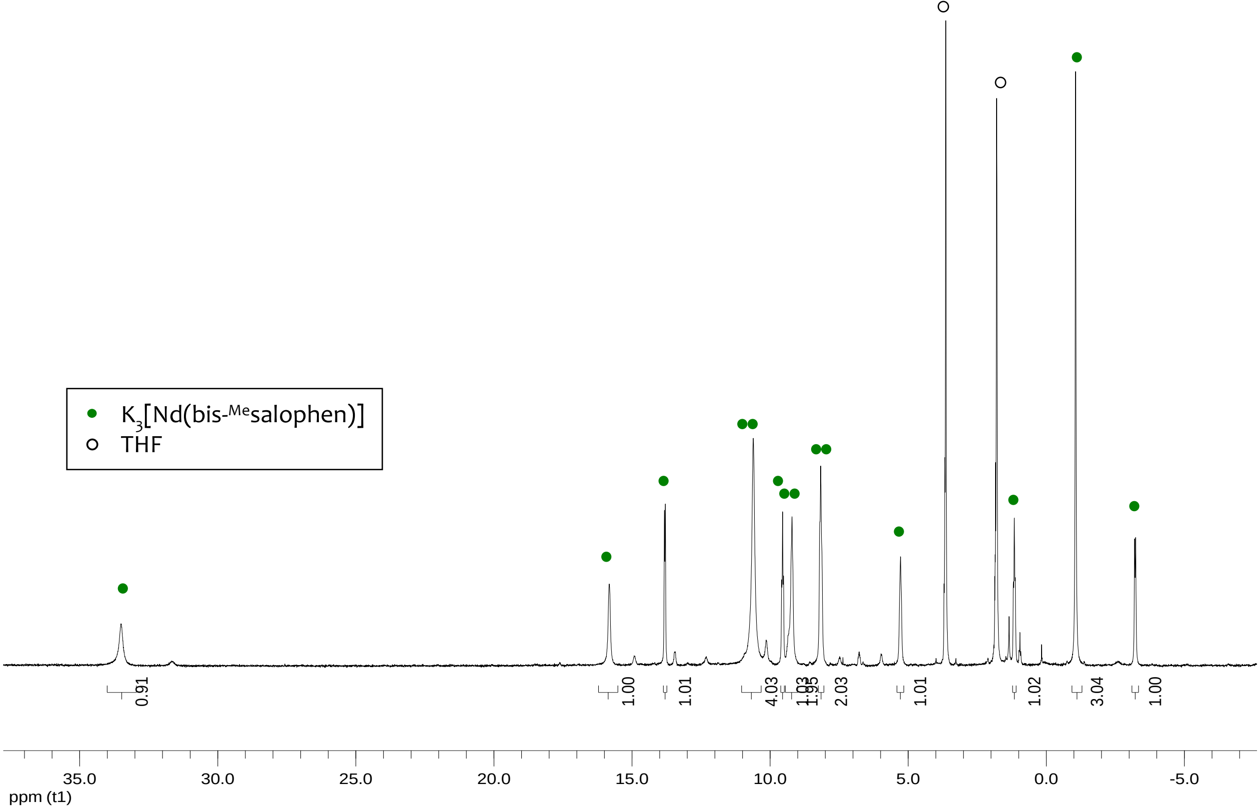

Figure S.B.15. ^{1}H NMR spectrum (298K, 400 MHz) in THF-d_8 of the complex **K[Nd(^{tBu}salophen)$_2$]**.

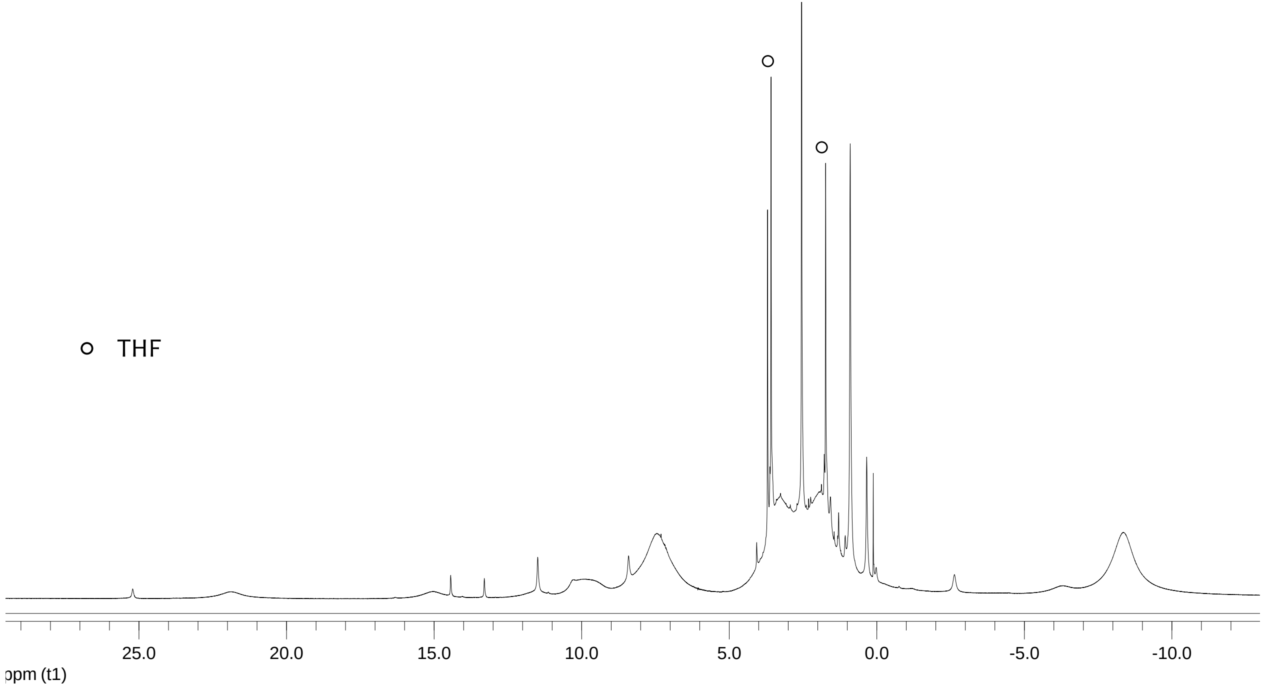

Figure S.B.16. ^{1}H NMR spectrum (298 K, 200 MHz) in THF-d_8 of the complex **K$_3$[Nd(bis-^{tBu}salophen)]**.

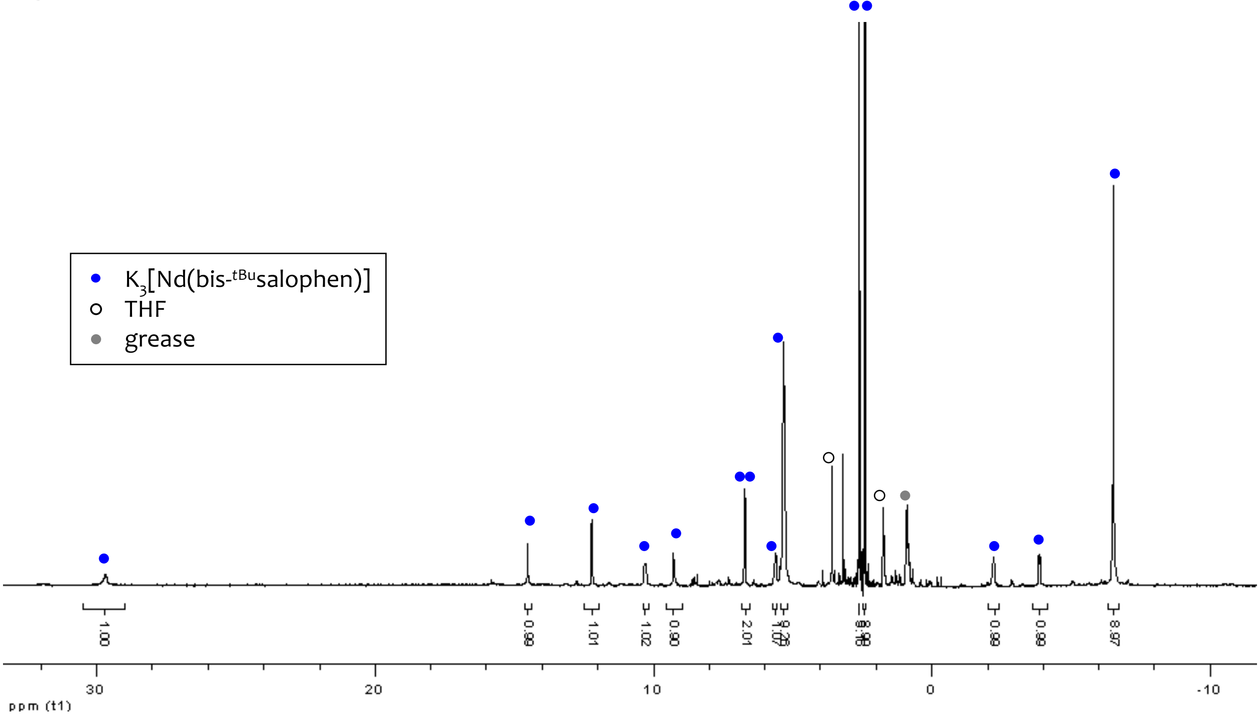

Figure S.B.17. ^{1}H NMR spectrum (243K, 400 MHz) in THF-d_8 of **K_3[Nd(bis-salophen)]** after reaction with two equivalents of AgOTf affording **K[Nd(salophen)$_2$]**.

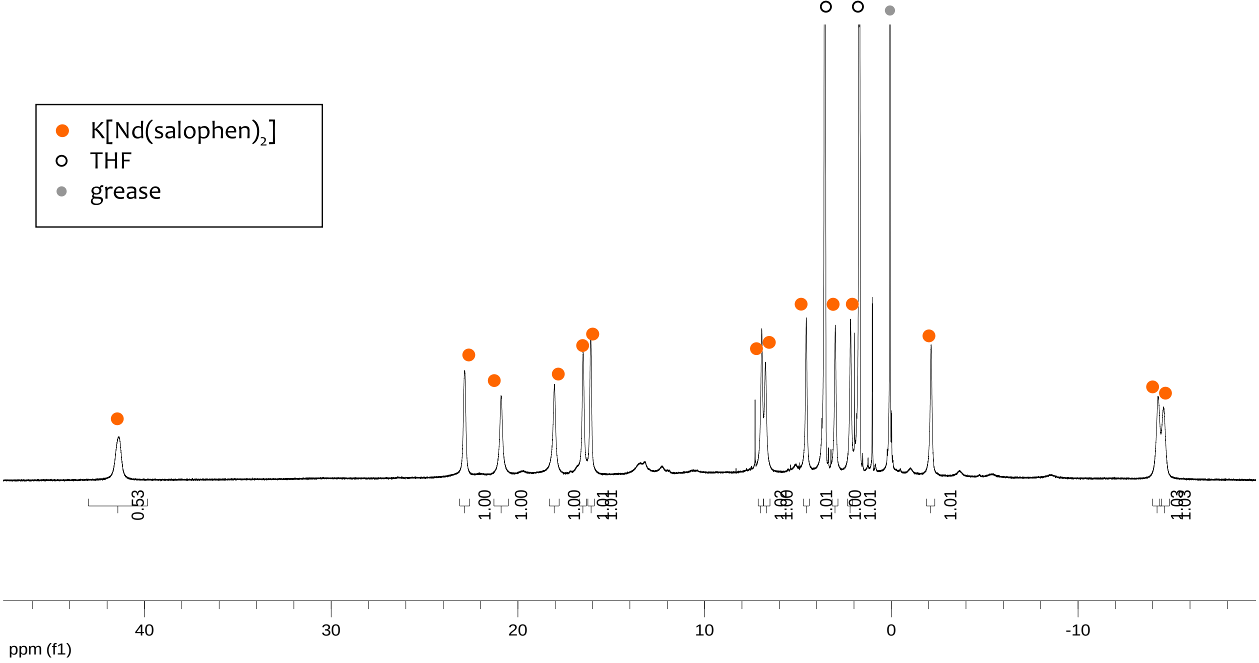

Figure S.B.18. ^{1}H NMR spectrum (298K, 400 MHz) in THF-d_8 of **K_3[Tb(bis-salophen)]** after reaction with two equivalents of AgOTf affording **K[Tb(salophen)$_2$]**.

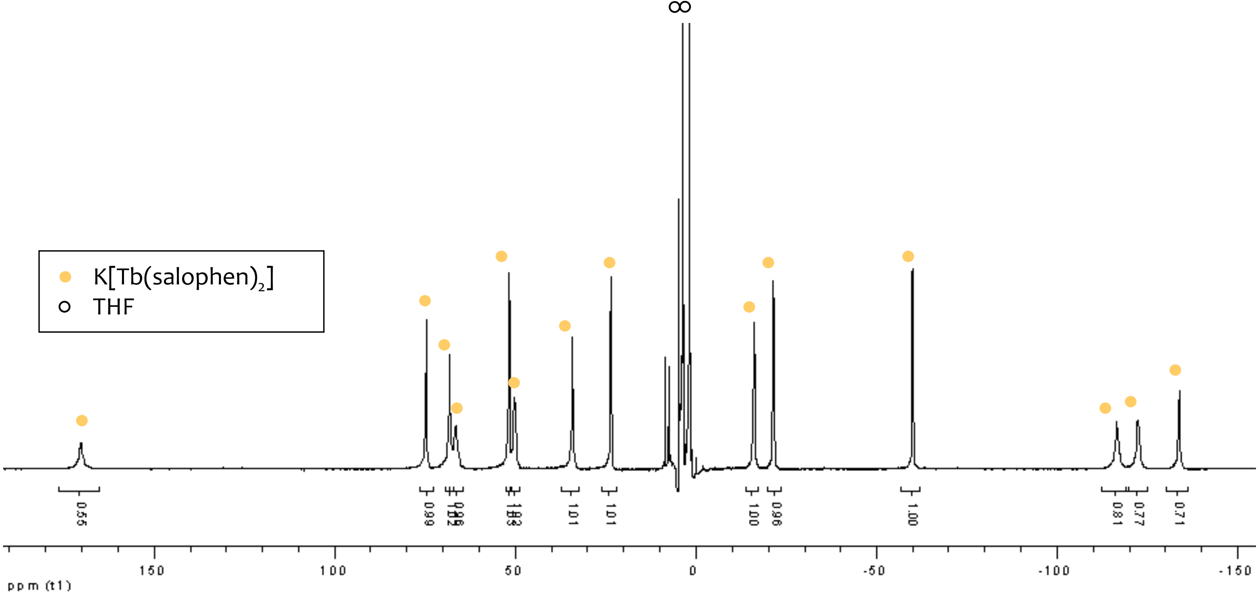

Figure S.B.19. ^{1}H NMR spectrum (243K, 400 MHz) in THF-d_8 of **K_3[Nd(bis-salophen)]** after reaction with one equivalent of 9,10-phenanthrenequinone affording **K[Nd(salophen)$_2$]**.

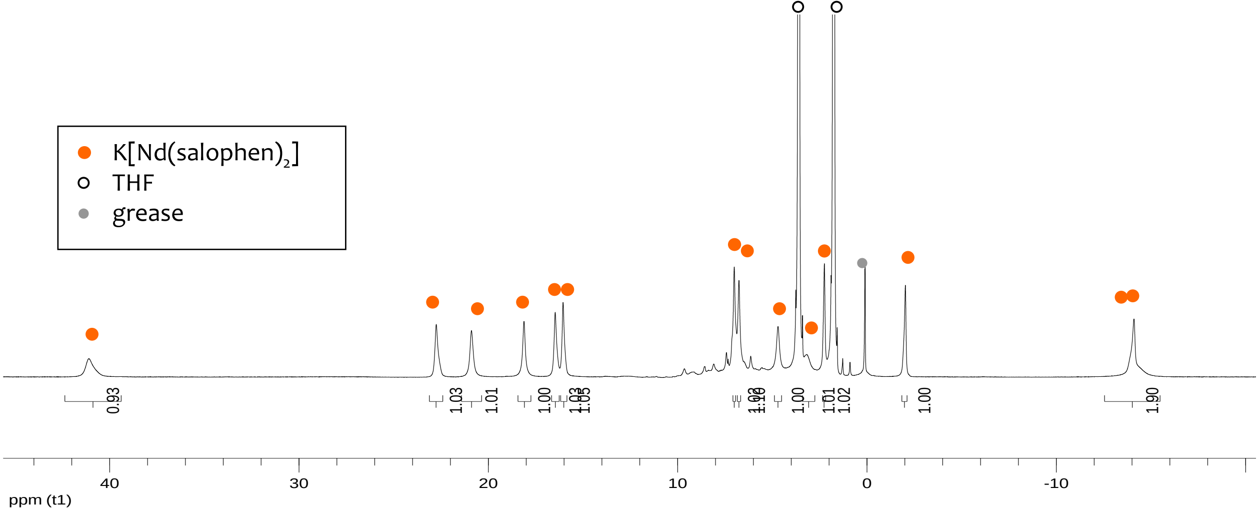

Figure S.B.20. ^{1}H NMR spectrum (243K, 400 MHz) in THF-d_8 of **K_3[Nd(bis-salophen)]** after reaction with one equivalents of I_2 affording **K[Nd(salophen)$_2$]**.

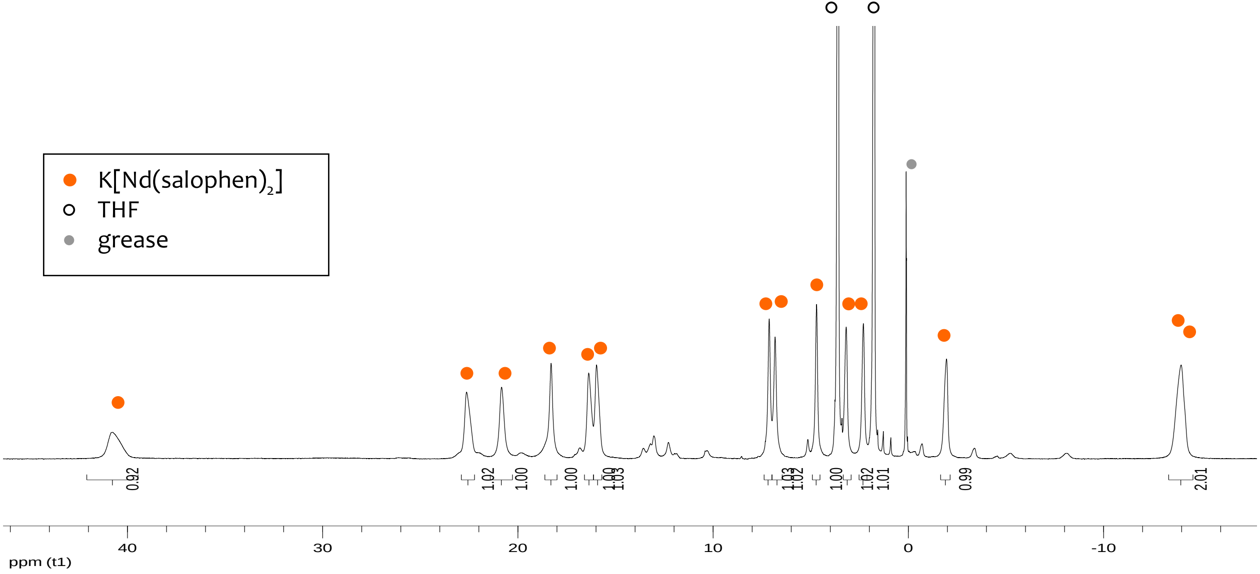

Figure S.B.21. ^{1}H NMR spectrum (243K, 400 MHz) in THF-d_8 of **K_3[Nd(bis-salophen)]** after reaction with dry oxygen affording **K[Nd(salophen)$_2$]** and **K_2salophen**.

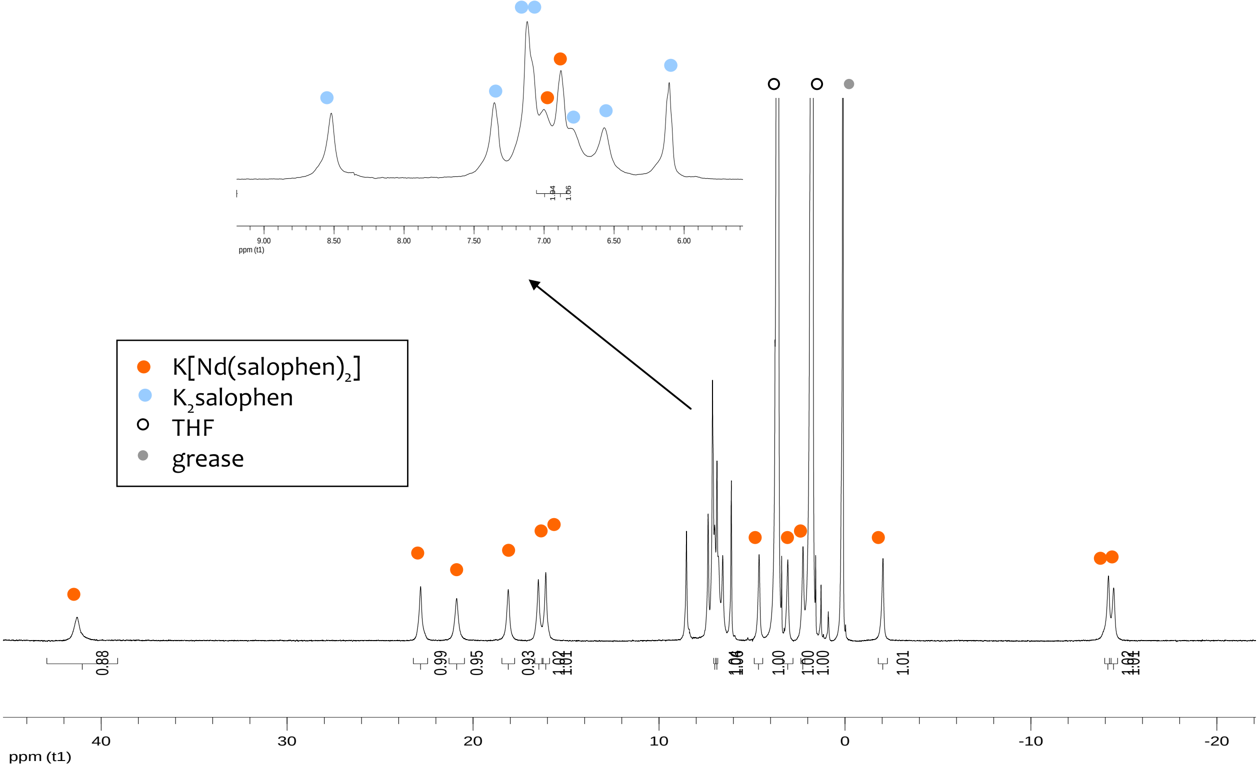

Figure S.B.22. ^{1}H NMR spectrum (298K, 200 MHz) in pyridine-d_5 of the complex **K[Nd(bis-H$_2$salophen)]**.

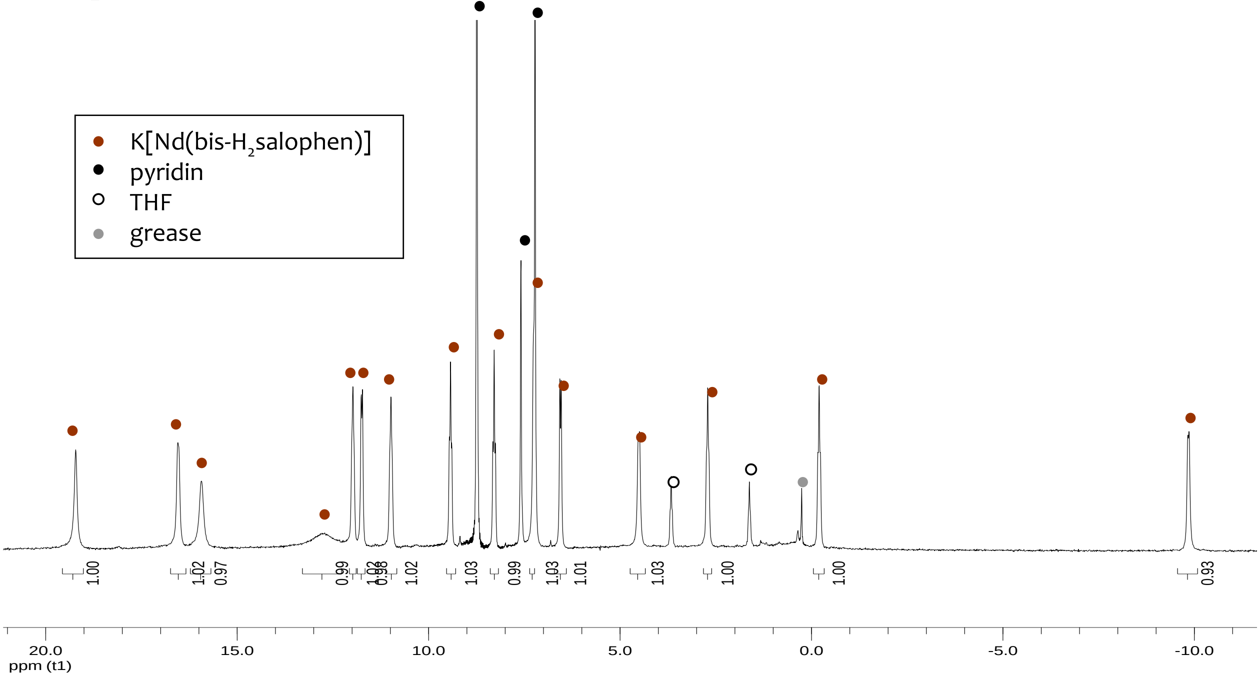

Figure S.B.23. ^{1}H NMR spectrum (298K, 200 MHz) in pyridine-d_5 of the crude reaction of 1 equivalent of K_2salophen with $NdI_3(THF)_4$. The same spectrum is obtained when the reaction is performed with $Nd(OTf)_3$.

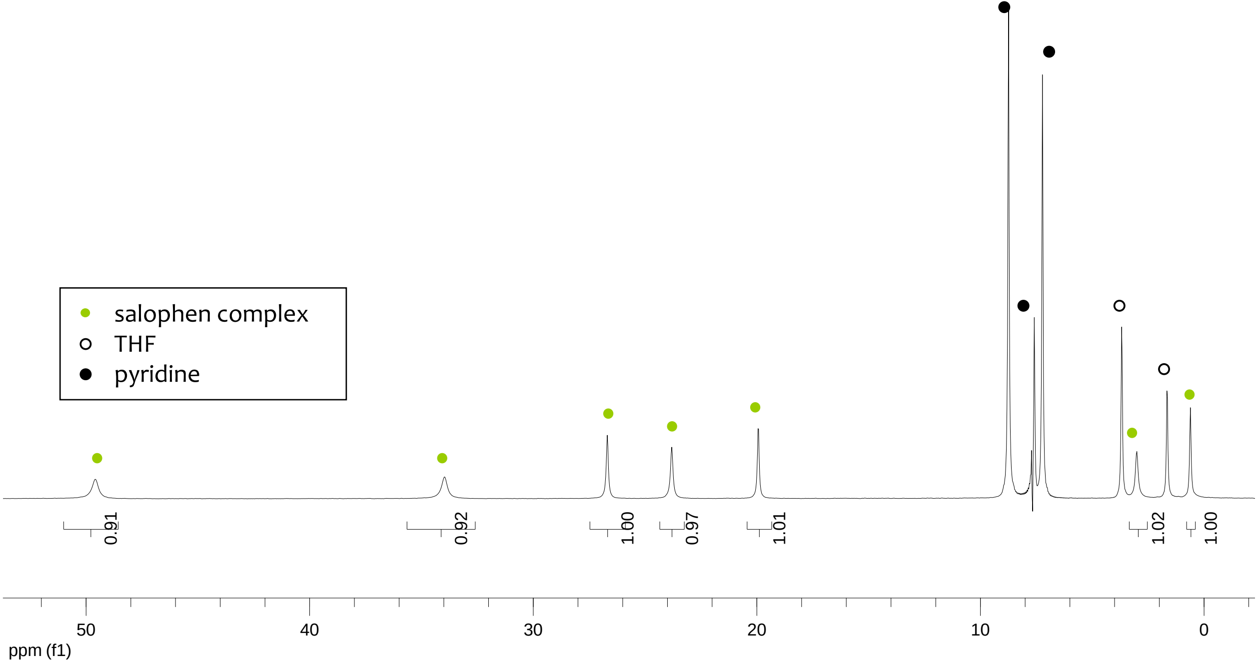

Figure S.B.24. ^{1}H NMR spectrum (298K, 200 MHz) in pyridine-d_5 of the crude mixture of the reaction of complex [**Nd_2(cyclo-salophen)]** with AgOTf.

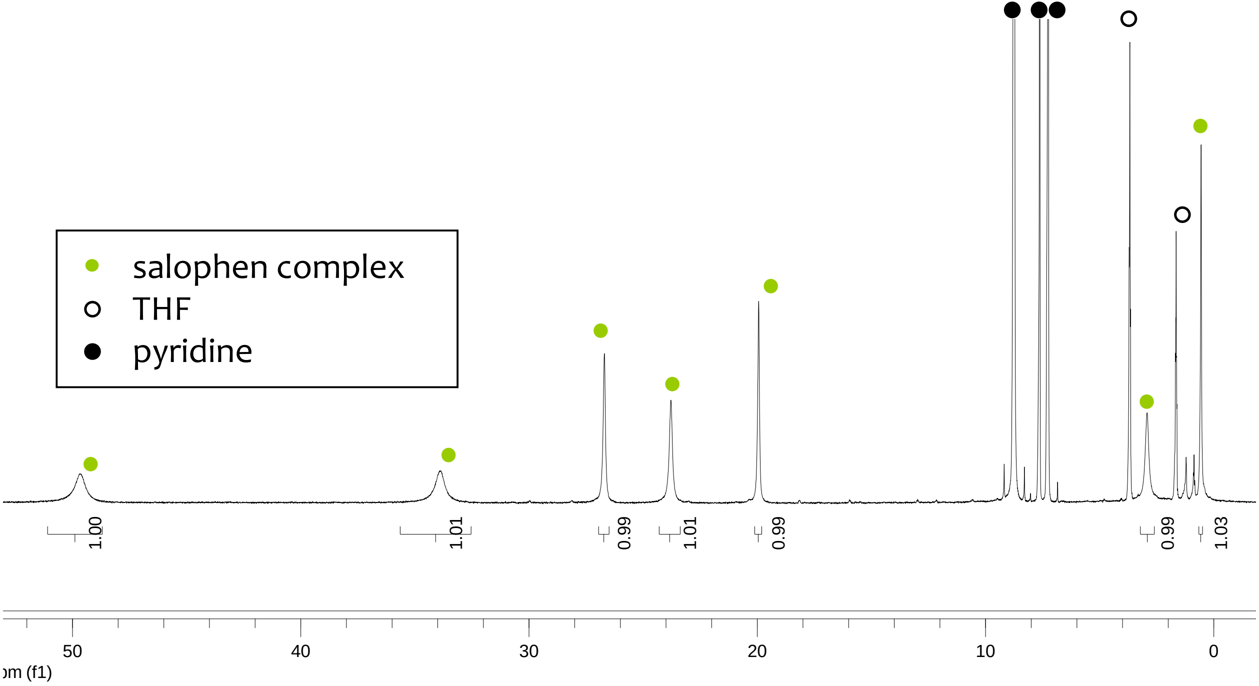

C) ES-MS spectra

Figure S.C.1. ESI mass spectrum (positive ionisation mode) of the complex **K[Nd(salophen)$_2$].**

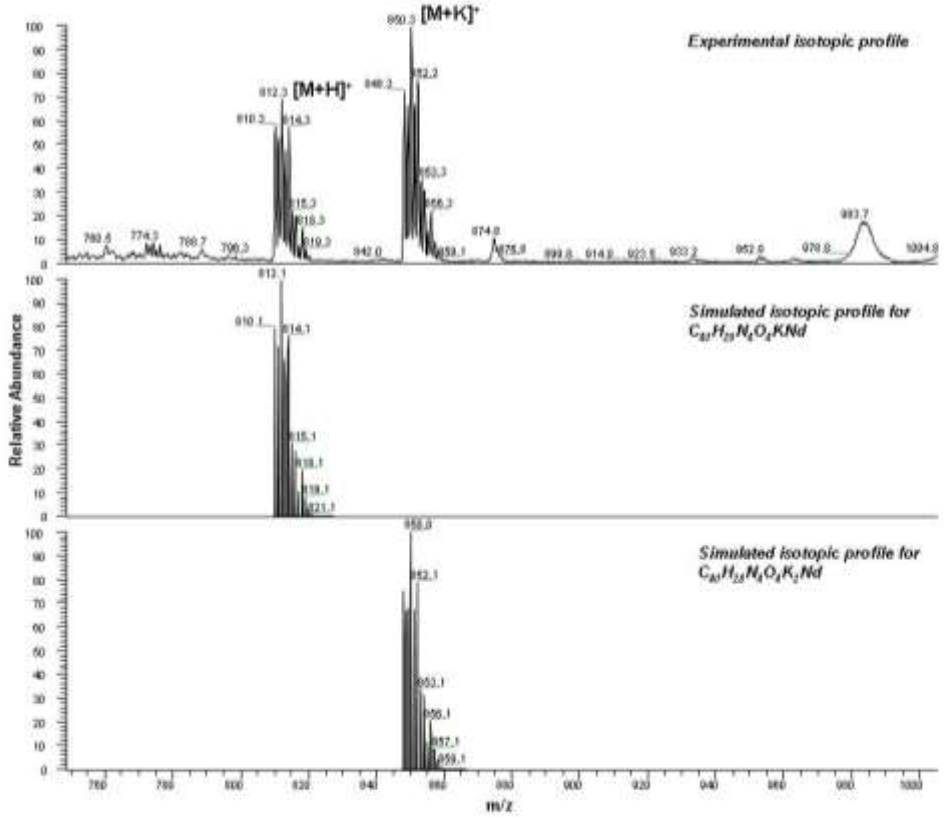

Figure S.C.2. ESI mass spectrum (positive ionisation mode) of the complex **K$_3$[Nd(bis-salophen)].**

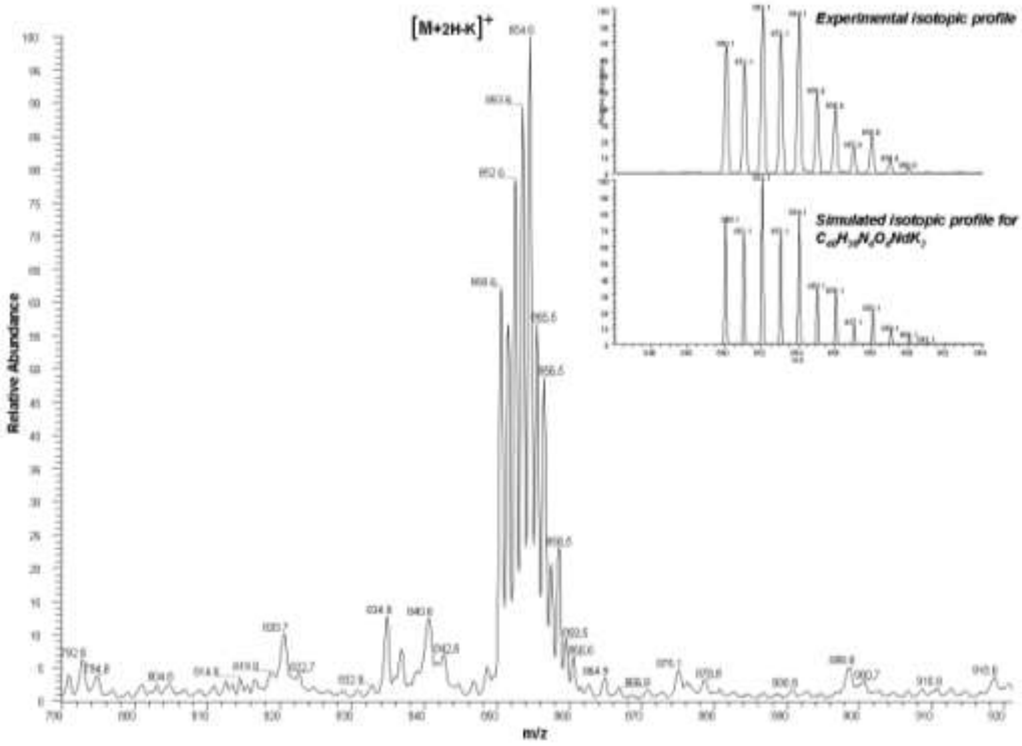

Figure S.C.3. ESI mass spectrum (positive ionisation mode) of the complex **K[Eu(salophen)$_2$].**

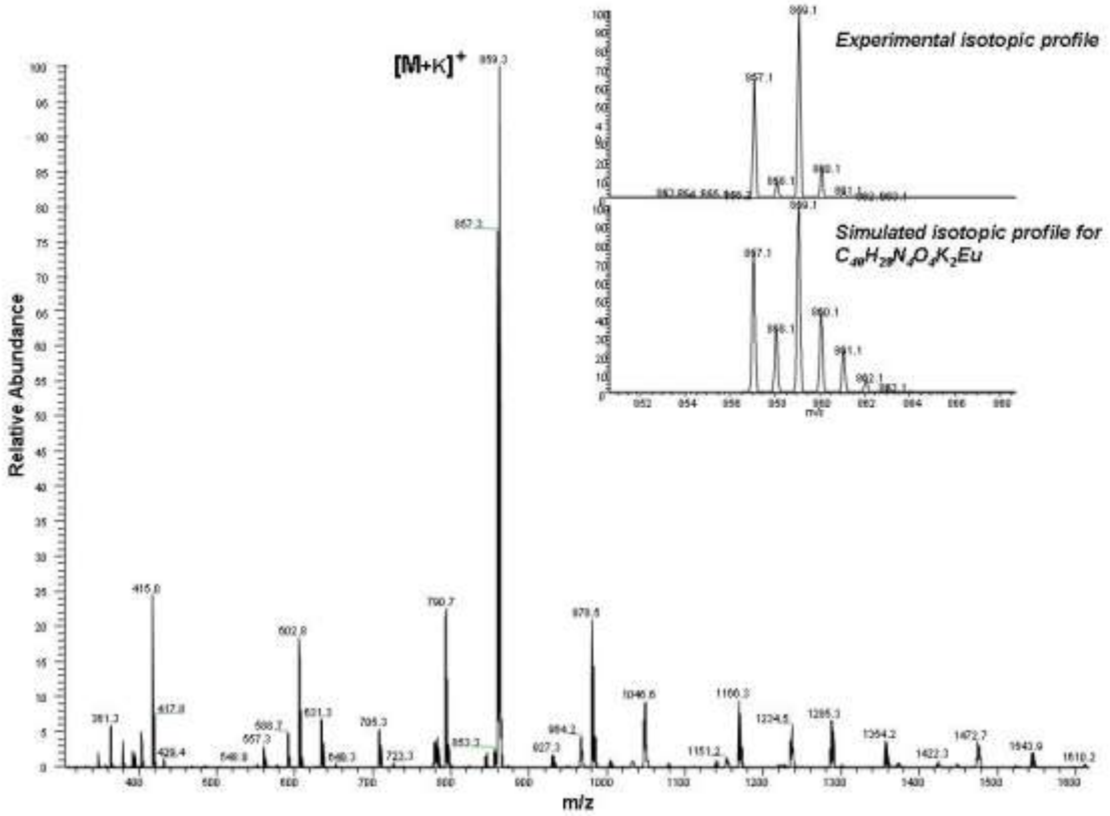

Figure S.C.4. ESI mass spectrum (positive ionisation mode) of the complex **K$_3$[Eu(bis-salophen)].**

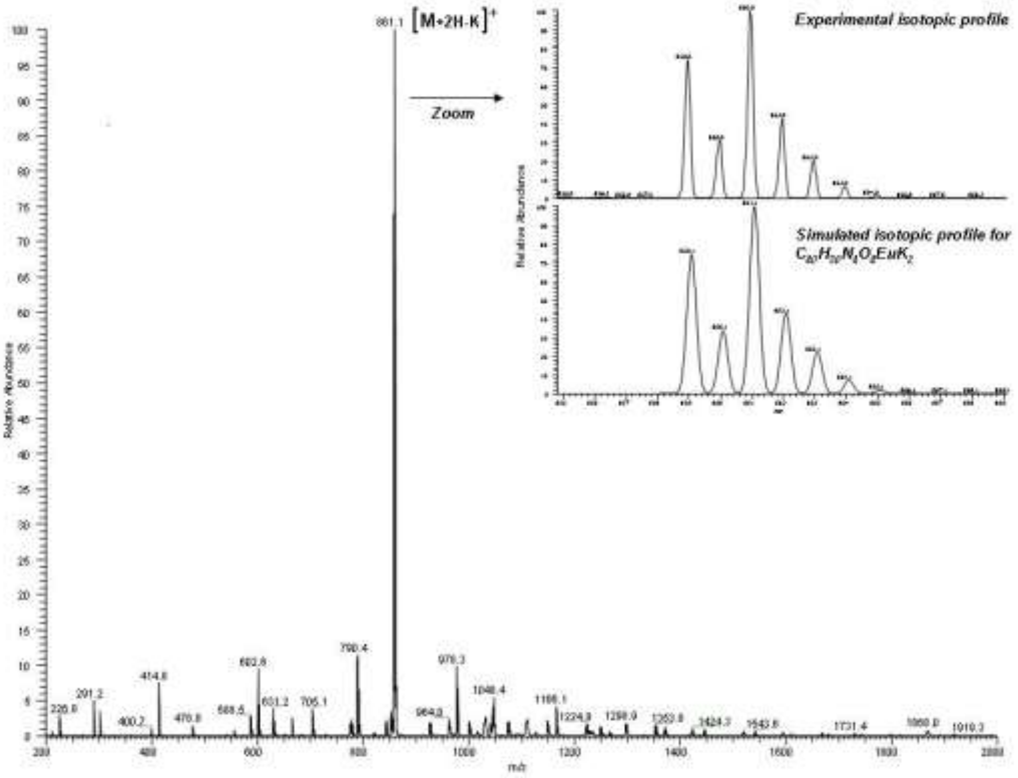

Figure S.C.5. ESI mass spectrum (positive ionisation mode) of the complex **K[Tb(salophen)$_2$].**

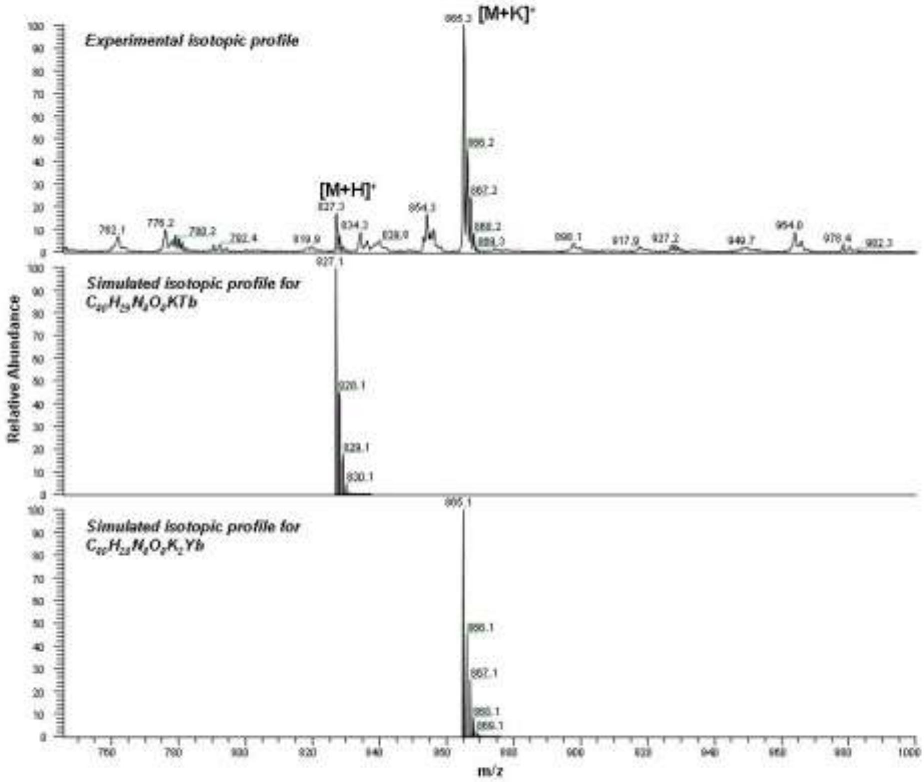

Figure S.C.6. ESI mass spectrum (positive ionisation mode) of the complex **K$_3$[Tb(bis-salophen)].**

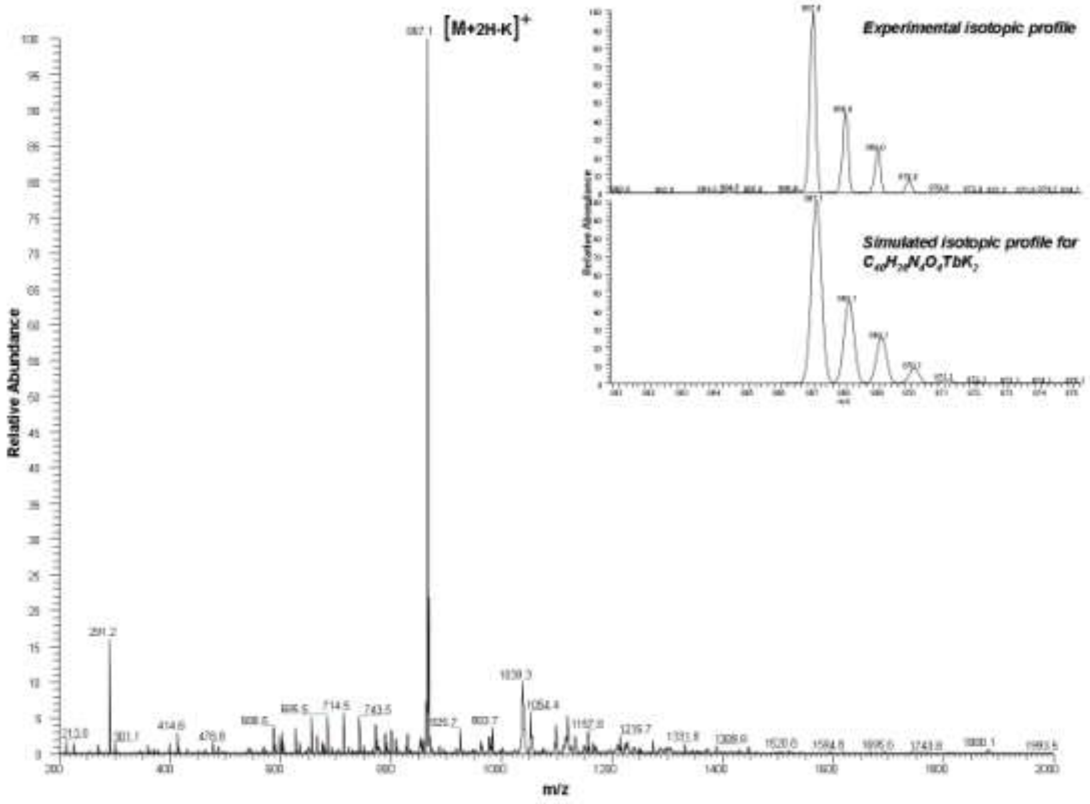

Figure S.C.7. ESI mass spectrum (positive ionisation mode) of the complex **K[Yb(salophen)$_2$].**

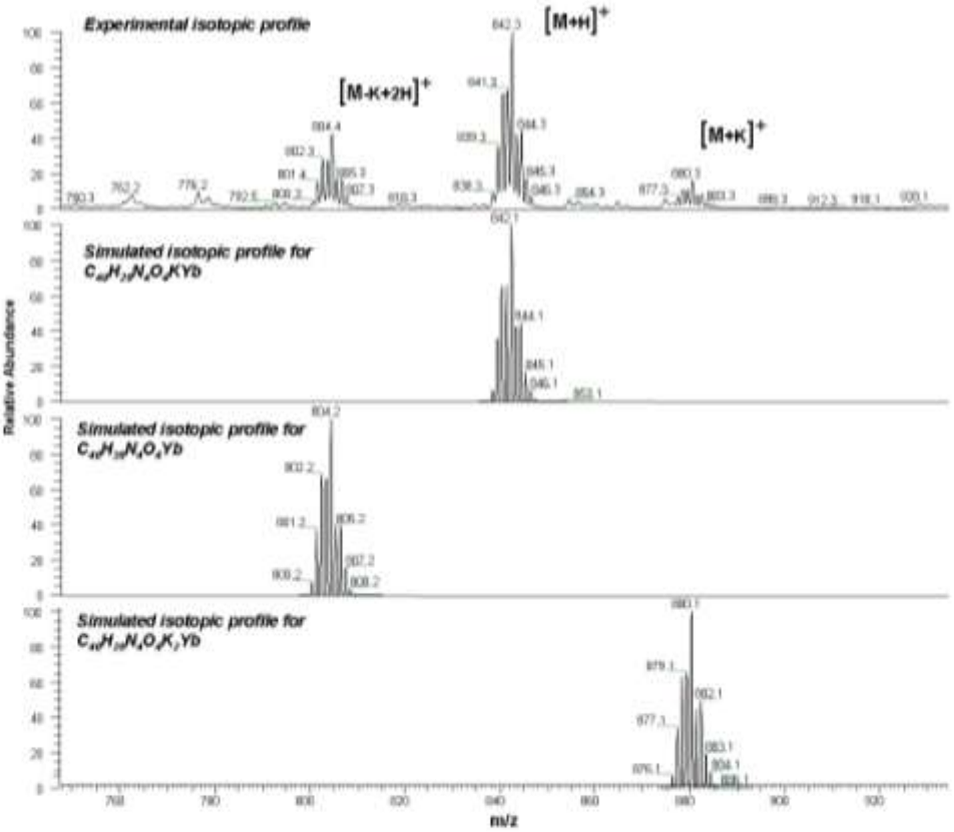

Figure S.C.8. ESI mass spectrum (positive ionisation mode) of the complex **K$_3$[Yb(bis-salophen)].**

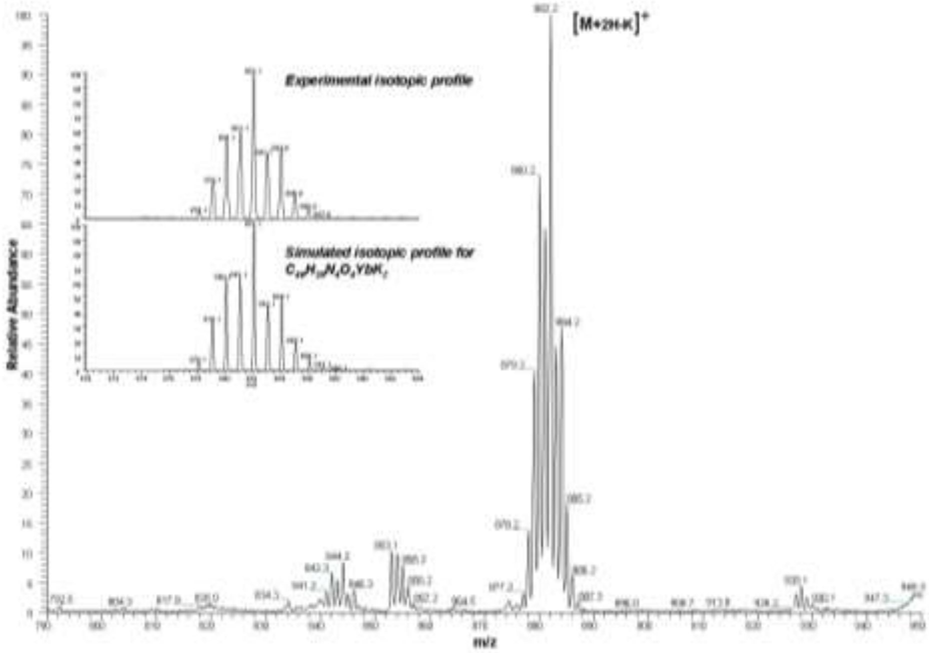

Figure S.C.9. ESI mass spectrum (positive ionisation mode) of the complex **K[Nd(^{Me}salophen)$_2$].**

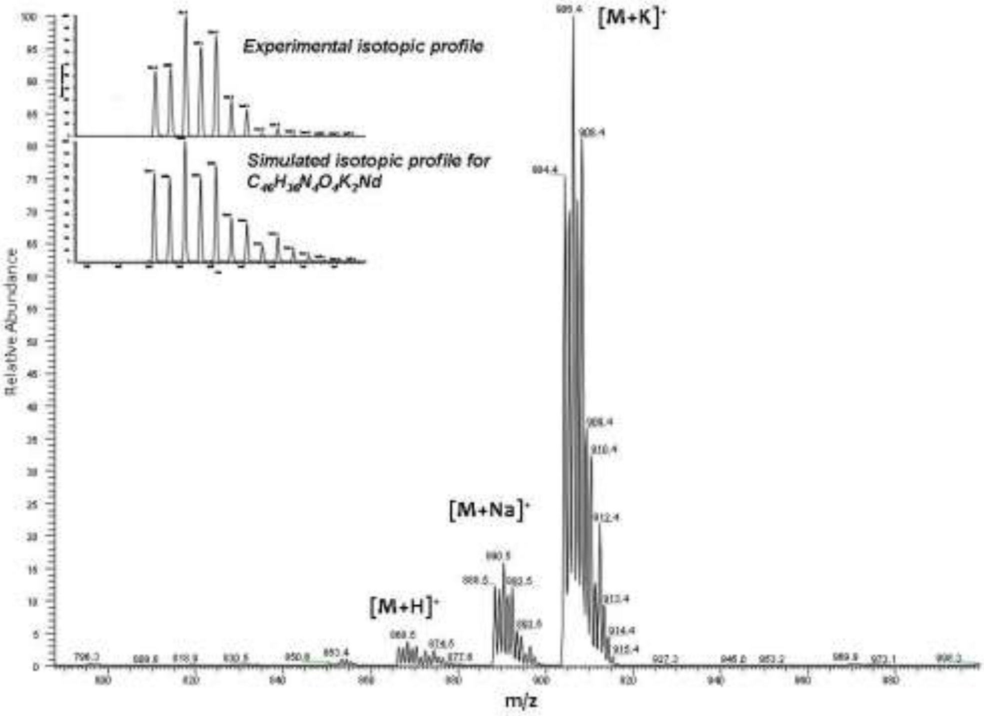

Figure S.C.10. ESI mass spectrum (negative ionisation mode) of the complex **K$_3$[Nd(bis-^{Me}salophen)].**

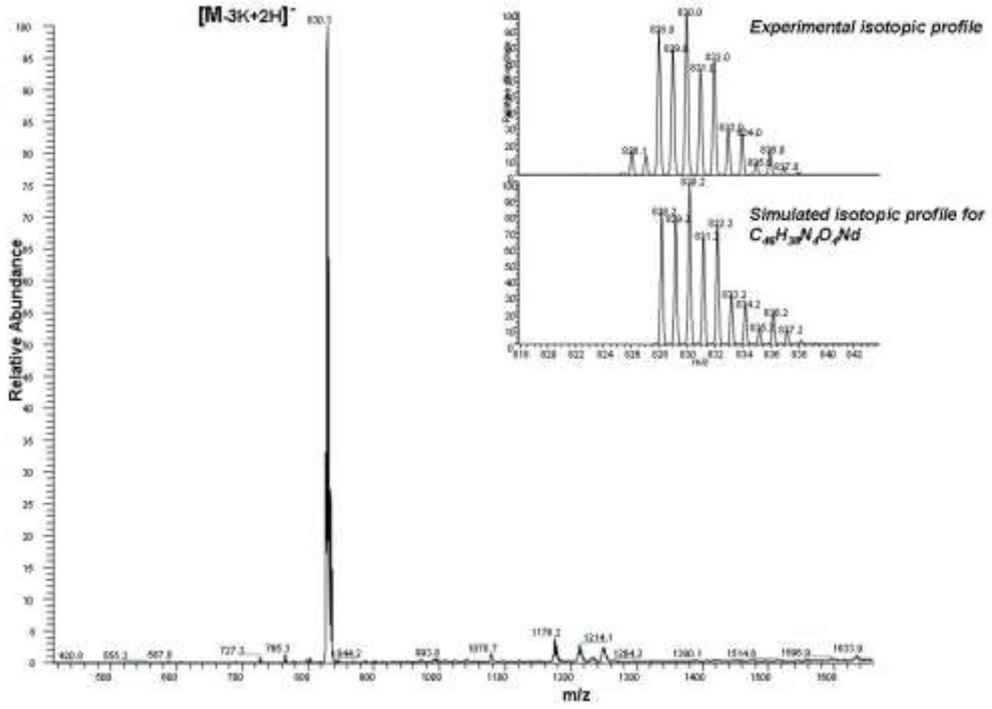

Figure S.C.11. ESI mass spectrum (negative ionisation mode) of the complex **K[Nd(^{tBu}salophen)$_2$]**.

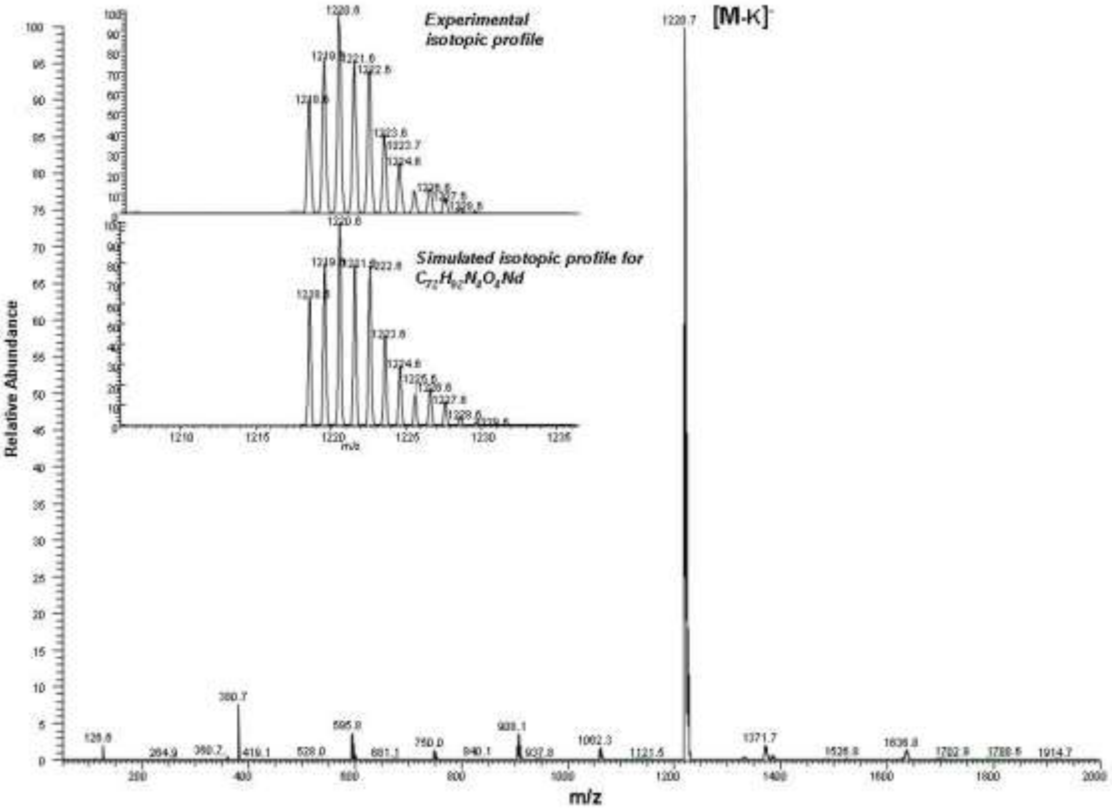

Figure S.C.12. ESI mass spectrum (negative ionisation mode) of the complex **K$_3$[Nd(bis-^{tBu}salophen)]**.

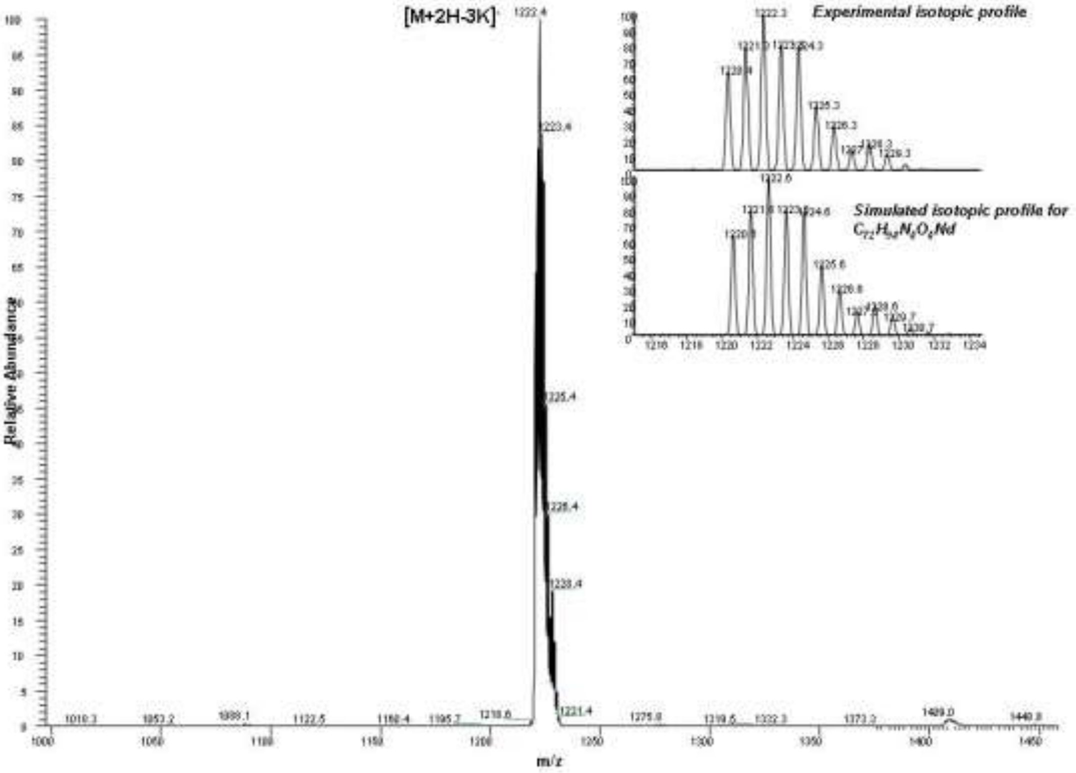

Figure S.C.13. ESI mass spectrum (positive ionisation mode) of the complex **K[Nd(bis-salophenH$_2$)].**

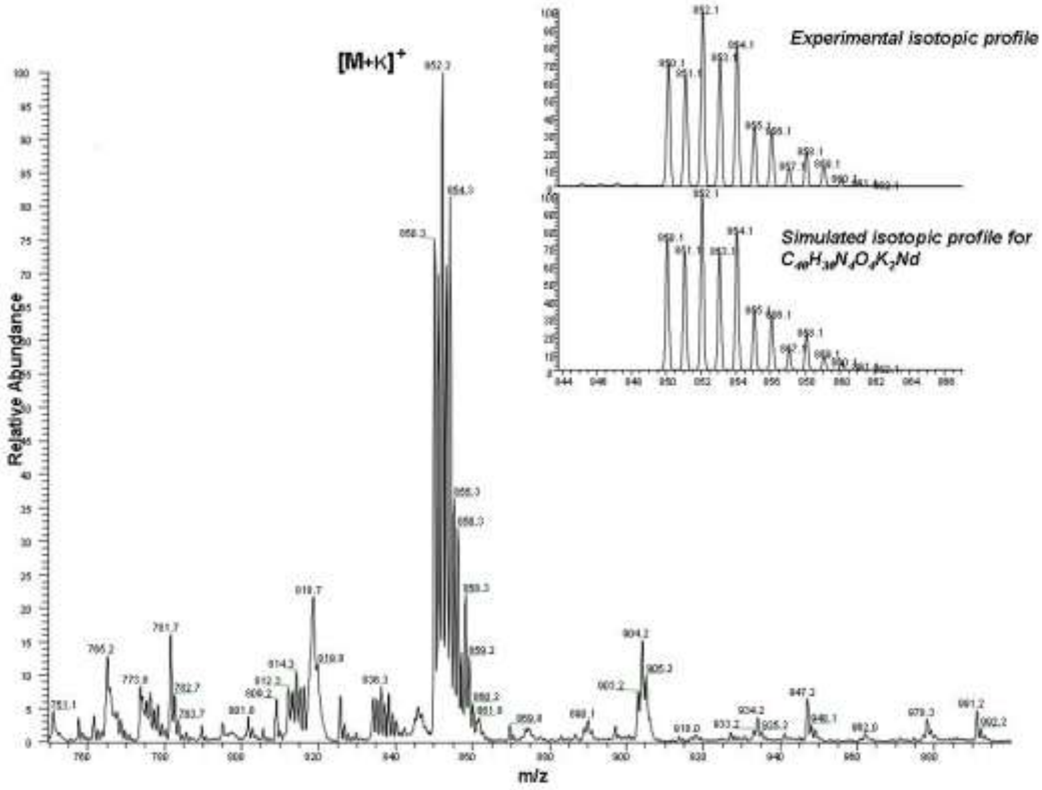

Figure S.C.14. ESI mass spectrum (positive ionisation mode) of the complex **K[Nd(salophen)$_2$]** formed from the reaction of 9,10-phenanthrenequinone with **K$_3$[Nd(bis-salophen)].**

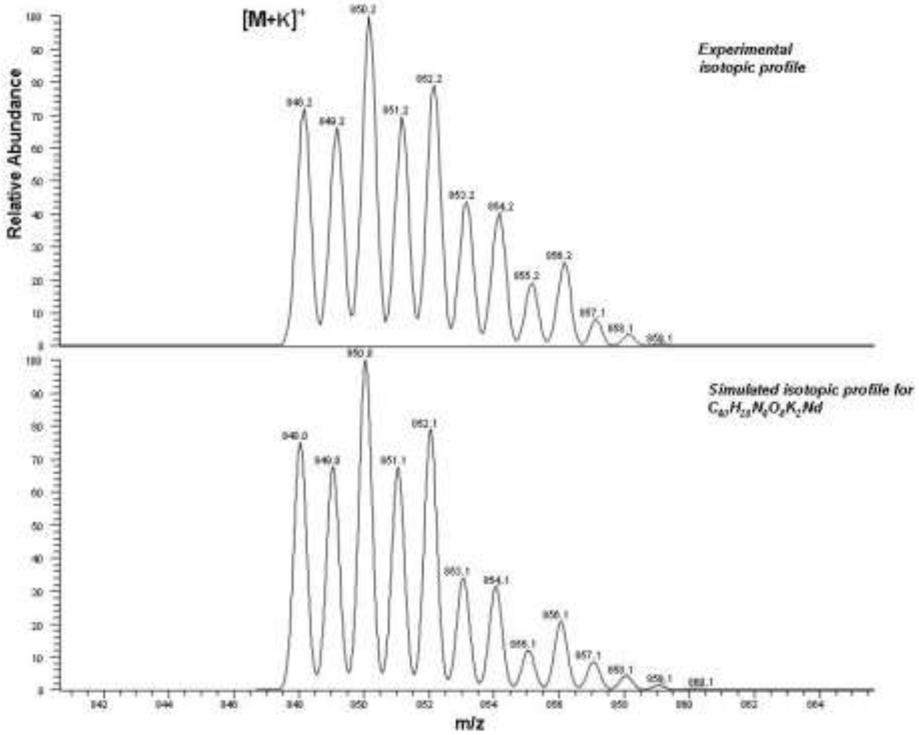

D) UV-vis spectra

Figure S.D.1. UV/visible spectra (298 K) of 0.5 mM THF solutions of complexes.

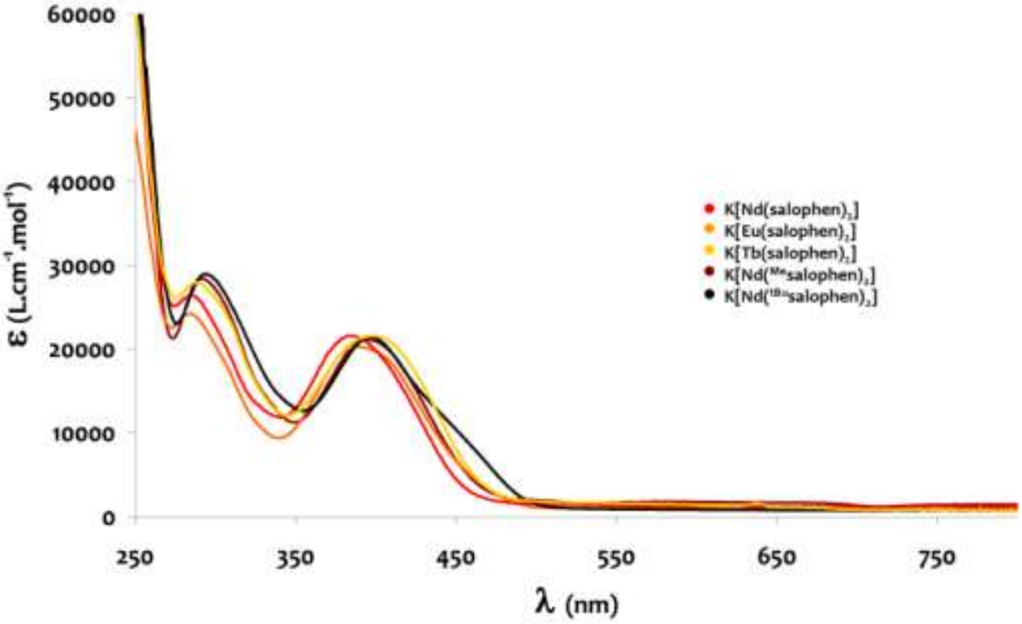

Figure S.D.2. UV/visible spectra (298 K) of 0.5 mM THF solutions of complexes.

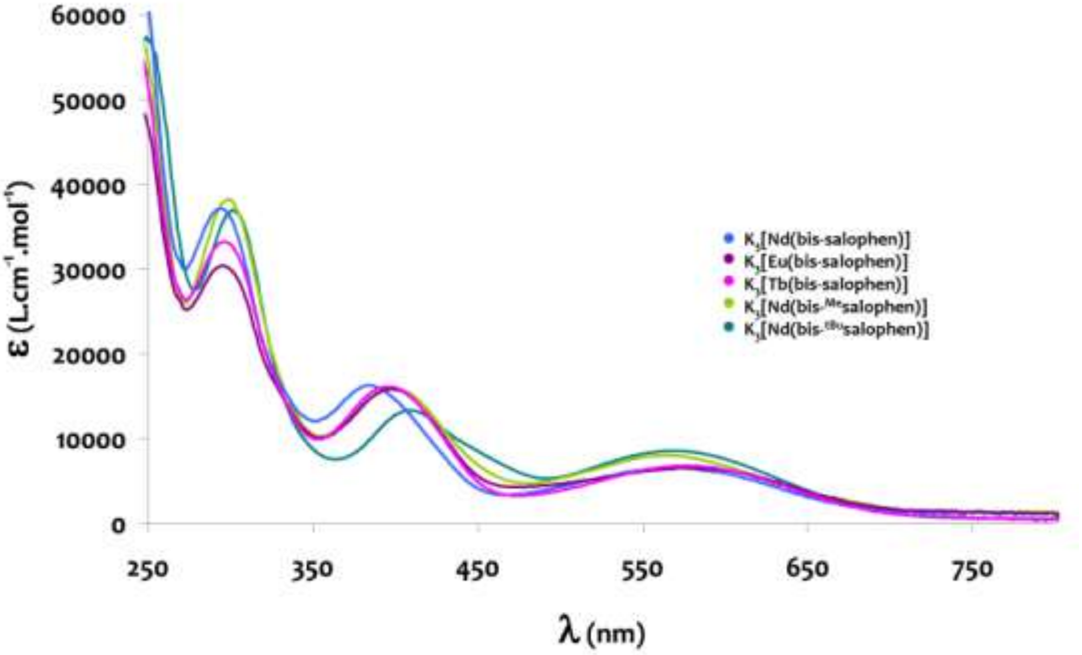

Figure S.D.3 UV/visible spectra (298 K) of 0.5 mM solutions of K_3[Nd(bis-salophen)] in various solvents showing an hypsochromic shift of the absorption band when the polarity of the solvent increase. Red : 1,4-Dioxane (λmax = 574 nm ; dielectric constant ε = 2.22 ; E_T = 36,0); Blue: Tetrahydrofuran (λmax = 567 nm ; dielectric constant ε = 7.52 ; E_T = 37,4); Green:Pyridine (λmax = 559 nm ; dielectric constant ε = 13.26 ; E_T = 40,2).

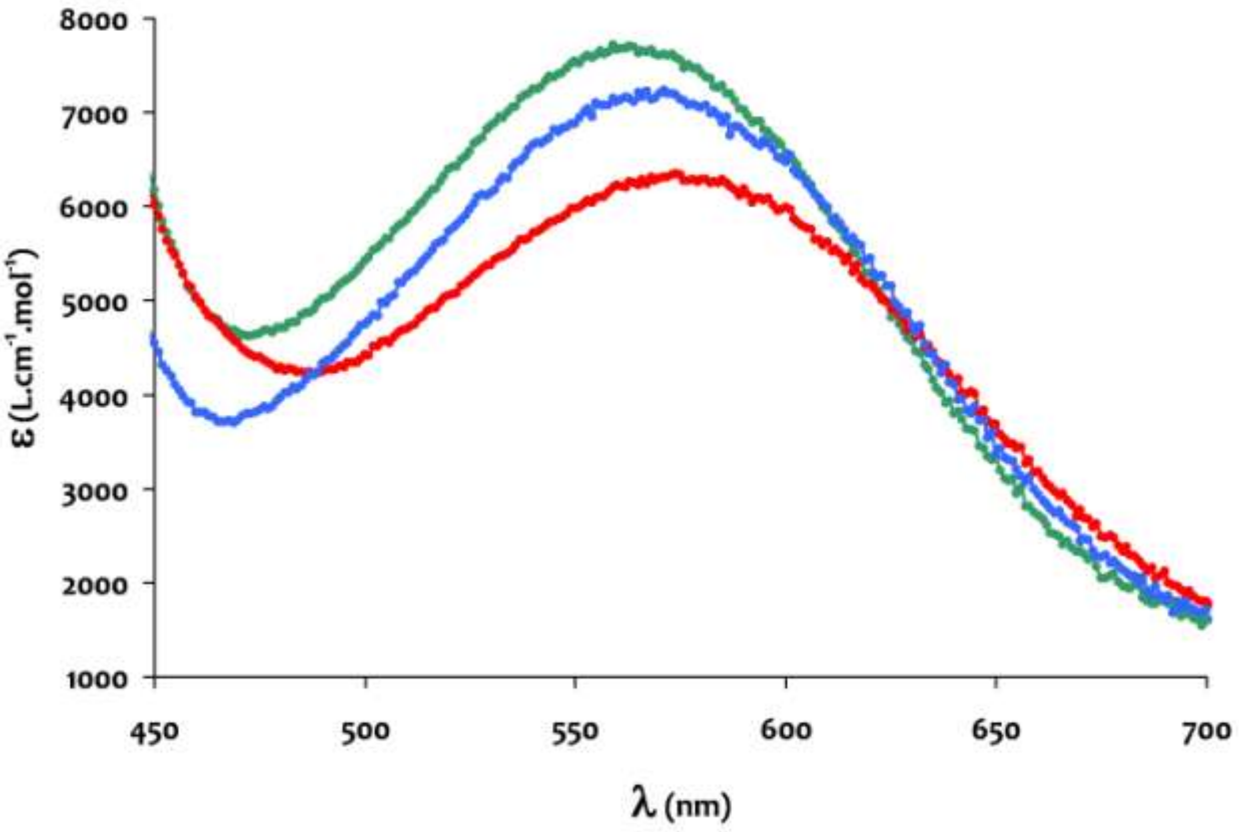

Figure S.D.4. UV/visible cells containing 0.5 mM THF solutions of K_3[Nd(bis-salophen)] (left) and K[Nd(salophen)$_2$] (right).

Figure S.D.5 UV/visible spectrum (298 K) of a 0.5 mM THF solution of complex $K_2[Nd_2(cyclo\text{-}salophen)(THF)_2]$.

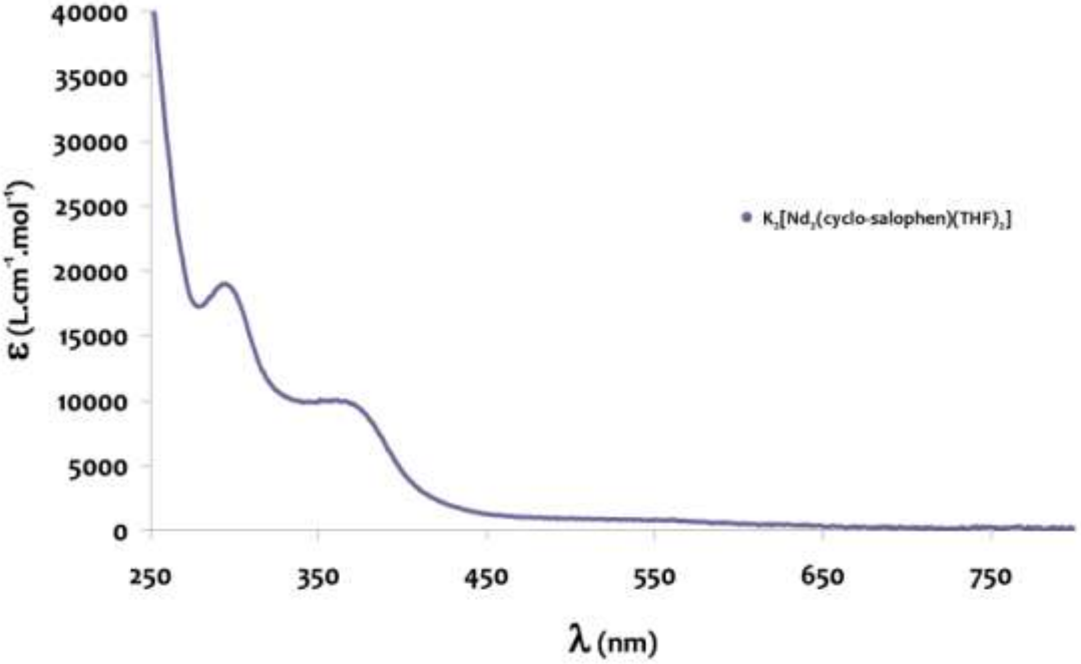

E) Electrochemistry

S.E.1) Determination of the number of electrons associated to the redox events

The number of electrons exchanged during the oxidation of complex K_3[Nd(bis-salophen)] was determined by the combination of a chronoamperometry experiment and a study of the stationary regime obtained at a platinum microelectrode.

A solution of K_3[Nd(bis-salophen)] and a solution of ferrocene (20 mM in complex with 0.1 M $[Bu_4N][PF_6]$ supporting electrolyte in pyridine) were prepared. A chronoamperometry study was carried out on both solutions using exactly the same experimental conditions (platinum disk (d = 5 mm) working electrode, platinum wire counter electrode and Ag/AgCl reference electrode).

The plot of the current i versus $t^{-1/2}$ (Figures S.E.1.1) obbey the Cottrell equation{ A. J. Bard and L. R. Faulkner, *Electrochemical Methods: Fundamentals and Applications*, John Wiley, New York, 2001}:

$$i = kt^{-1/2} \text{ with } k = nFACD^{1/2}(\pi)^{-1/2}$$

where i is the current, n the number of electrons, F the Farraday constant, A the electroactive area of the electrode, D the diffusion coefficient of the species and t the time.

As the concentration of the ferrocene solution is equal to the one of the K_3[Nd(bis-salophen)] solution, and as the number of electrons involved in the oxidation of ferrocene is 1, the ratio of the director coefficient k of the plot measured for the ferrocene and the K_3[Nd(bis-salophen)] solutions is :

$$k_{Nd}/k_{Fc} = n(D/D')^{1/2}$$

where D' is the diffusion coefficient for ferrocene, D is the diffusion coefficient for K_3[Nd(bis-salophen)] and n is the number of electrons involved in the oxidation of K_3[Nd(bis-salophen)].

Figure S.E.1.1 i vs $t^{-1/2}$ plot of the chronoamperometry data obtained from a 20 mM ferrocene solution (blue diamonds) and a 20 mM K_3[Nd(bis-salophen)] (red diamonds) in a 0.1 M $[Bu_4N][PF_6]$ pyridine solution.

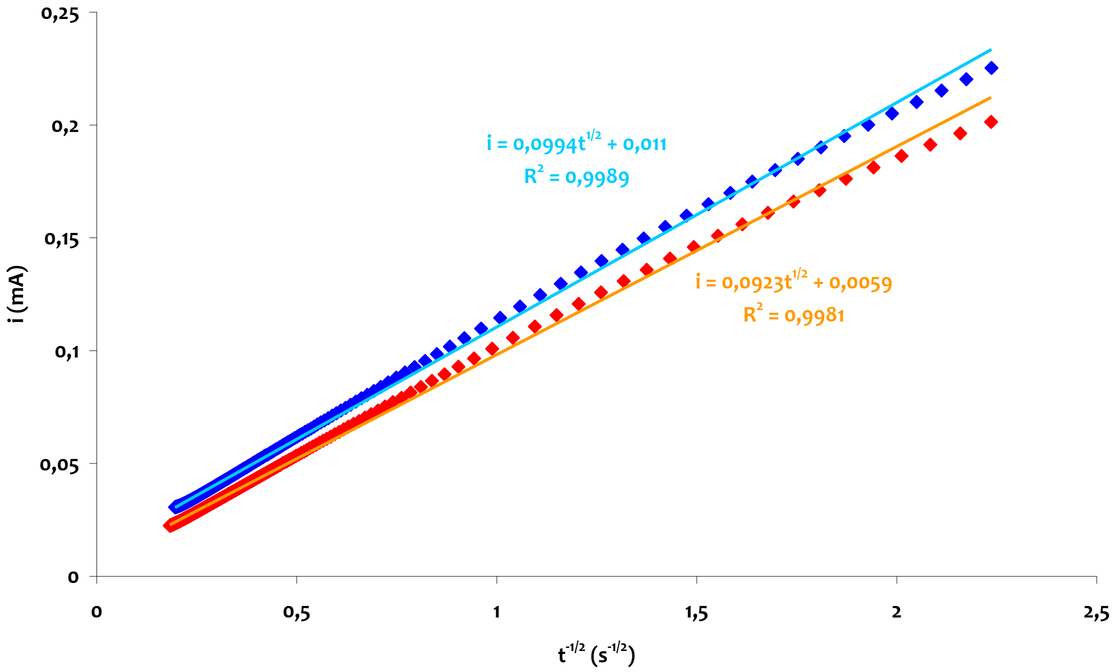

In parallel, the intensity of the current at a microelectrode in stationnary regime was measured for both solutions (Figure S.E.1.2). The value of the limiting current is given by the following relation:

$$i^{lim} = 4nFrCD$$

where i is the current, n the number of electrons, F the Farraday constant, D the diffusion coefficient of the species, r the radius of the platinum microdisk and C the concentration of the complex in the bulk solution.

Similarly, the ratio of the limit intensities measured for the ferrocene and the K_3[Nd(bis-salophen)] solutions is :

$$i^{lim}_{Nd}/i^{lim}_{Fc} = nD/D'$$

where D' is the diffusion coefficient for ferrocene, D is the diffusion coefficient for K_3[Nd(bis-salophen)] and n is the number of electrons involved in the oxidation of K_3[Nd(bis-salophen)].

Figure S.E.1.2 i vs E plot of a 20 mM ferrocene solution (blue curve) and a 20 mM K_3[Nd(bis-salophen)] (red curve) in a 0.1 M $[Bu_4N][PF_6]$ pyridine solution obtained in stationnary regime at a platinum microdisk (0,5 mV/s scan rate).

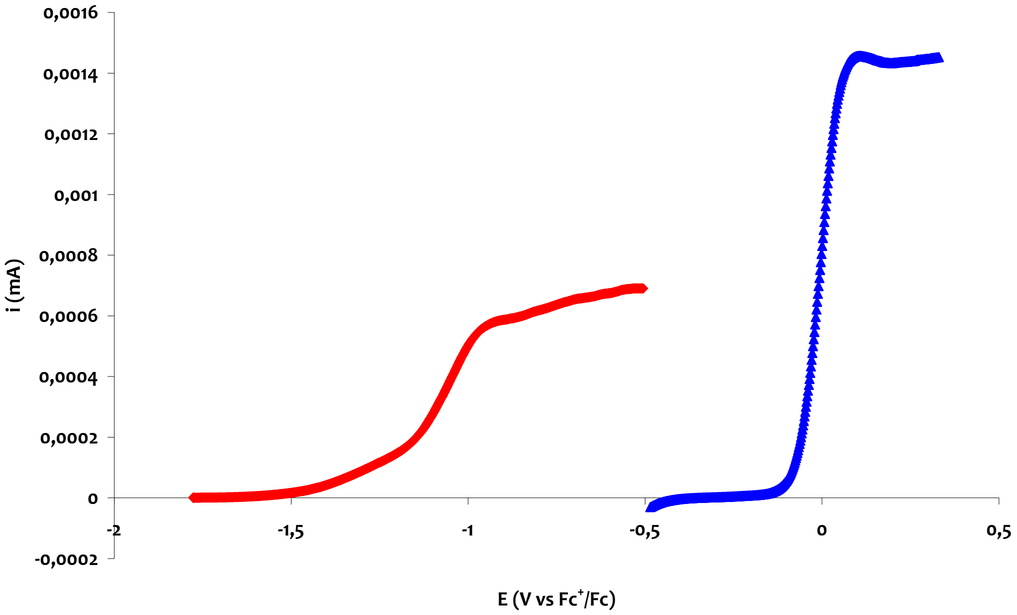

The number of electrons exchanged during the oxidation of complex K_3[Nd(bis-salophen)] is then given by:

$$n = (k_{Nd}/k_{Fc})^2/(i^{lim}_{Nd}/i^{lim}_{Fc}).$$

From our data (Table S.E.1.1), we find **n = 1.9±0.1**
Accordingly, the process observed by electrochemistry for the oxidation of the bis-salophen ligand involves a **transfer of 2 electrons.**

Table S.E.1.1 Electrochemistry data.

k_{Nd} (mA.s$^{1/2}$)	k_{Nd} (mA.s$^{1/2}$)	i^{lim}_{Nd} (µA)	i^{lim}_{Fc} (µA)	n
0.092	0.099	0.65	1.44	1.9

S.E.2) Scan-rate studies:

Figure S.E.2.1 Scan-rate effect on the cyclovoltammogram of a 20mM solution of K_3[Nd(bis^{Me}salophen)] in pyridine performed with a microdisc platinum working electrode. Scan-rate range: 10mV/s (blue) to 1000 mV/s (yellow). Insert: Plot of the anodic peak current (i_{pA}) versus the square-root of the scan-rate ($v^{1/2}$) (v = 10 to 10000 mV/s). The linear variation of the peak current with the square-root of the scan rate is in agreement with the Randles-Sevcik equation.{ A. J. Bard and L. R. Faulkner, *Electrochemical Methods: Fundamentals and Applications*, John Wiley, New York, 2001.}

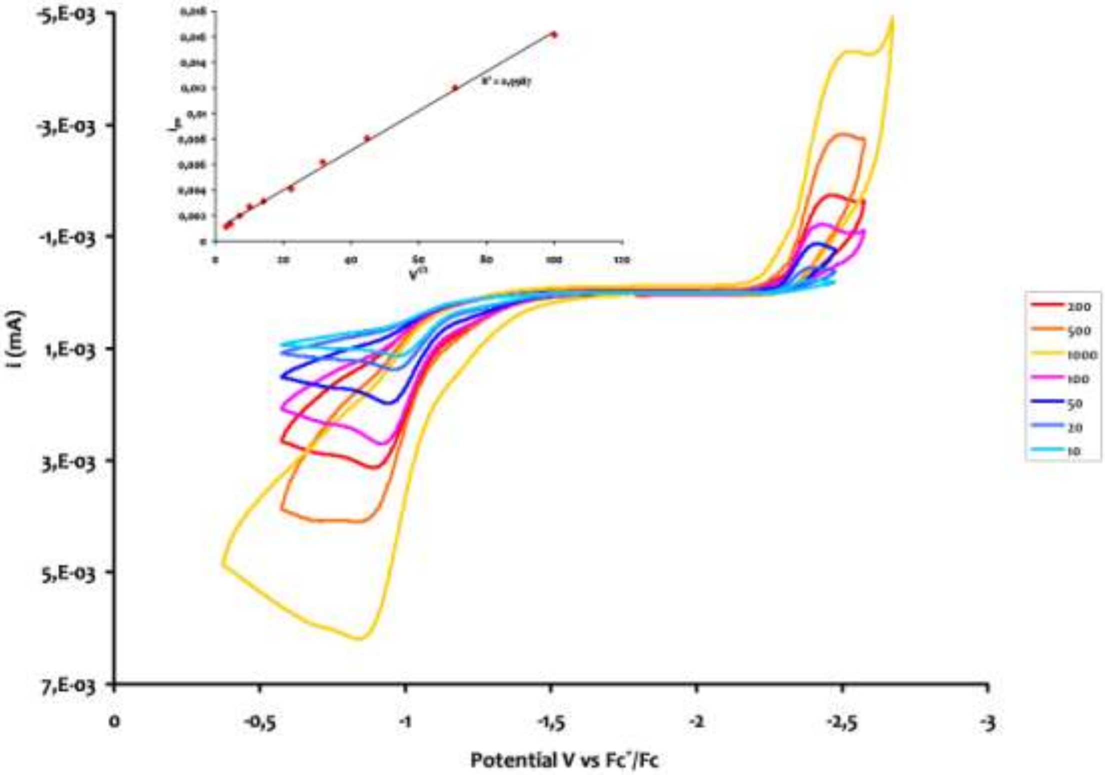

Figure S.E.2.2 Fast-scan cyclovoltammogram of a 20mM solution of K_3[Nd(bis^{Me}salophen)] in pyridine performed with a microdisc platinum working electrode. Scan-rate range: 5000mV/s (dark green) to 50000 mV/s (light green).

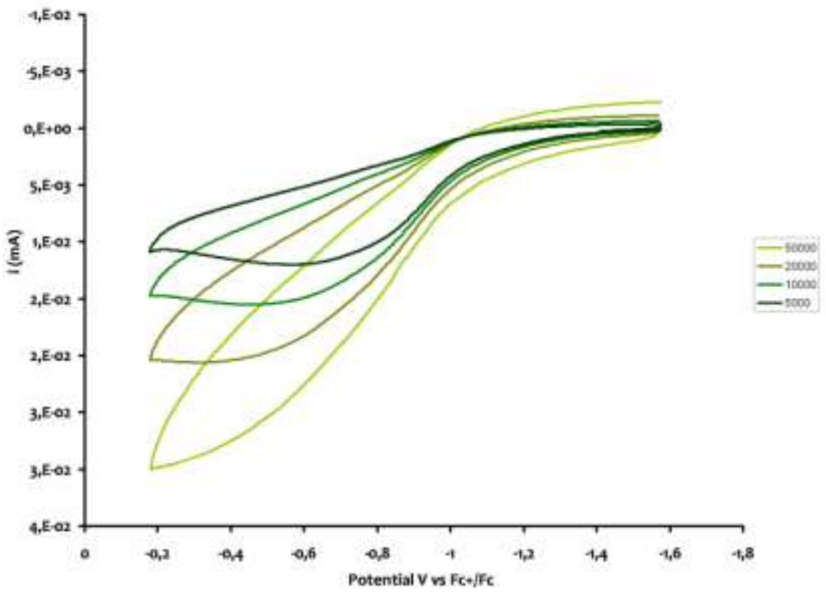

No reversibility could be detected in the scan-rate range 10mV/s to 50000mV/s. For fast-scan studies, even when using a microelectrode, the signal is affected by the IR drop, but does not show any reversibility.